NASA CONTRACTOR REPORT

NASA CR-2059

A FAST-ACTING ELECTRICAL SERVO FOR THE ACTUATION OF FULL-SPAN, FOWLER-TYPE WING FLAPS IN DLC APPLICATIONS

A Detail Design Study

by Frederick O. Smetana, Rafael J. Montoya, and Ronald K. Carden

Prepared by
NORTH CAROLINA STATE UNIVERSITY
Raleigh, N. C.
for Langley Research Center

NATIONAL AERONAUTICS AND SPACE ADMINISTRATION • WASHINGTON, D. C. • JULY 1972

1. Report No.	2. Government Accession No.	3. Recipient's Catalog No.
NASA CR-2059		

4. Title and Subtitle	5. Report Date
A Fast-Acting Electrical Servo for the Actuation of Full-Span, Fowler-Type Wing Flaps in DLC Applications - A Detail Design Study	JULY 1972
	6. Performing Organization Code
7. Author(s)	8. Performing Organization Report No.
Frederick O. Smetana, Rafael J. Montoya, and Ronald K. Carden	
9. Performing Organization Name and Address	10. Work Unit No.
North Carolina State University Raleigh, N.C.	736-05-10-01
	11. Contract or Grant No.
	NGR 34-002-086
12. Sponsoring Agency Name and Address	13. Type of Report and Period Covered
National Aeronautics and Space Administration Washington, D.C. 20546	Contractor Report
	14. Sponsoring Agency Code

15. Supplementary Notes

16. Abstract

The philosophy and detail design of an electro-mechanical actuator for Fowler-type wing flaps which have a response time constant of 0.025 seconds are described. A conventional electrical servomotor with a power rating twice the maximum power delivered to the load is employed along with adaptive, gain-scheduled feedback and various logic circuits, including one to remove electrical excitation from the motor during extended periods when no motion of the flap is desired.

17. Key Words (Suggested by Author(s))	18. Distribution Statement
Electro-mechanical actuator Compensation loops Gain scheduling System responses	Unclassified - Unlimited

19. Security Classif. (of this report)	20. Security Classif. (of this page)	21. No. of Pages	22. Price*
Unclassified	Unclassified	87	$3.00

*For sale by the National Technical Information Service, Springfield, Virginia 22151

TABLE OF CONTENTS

TABLE OF CONTENTS (continued) Page

LIST OF TABLES

LIST OF FIGURES

LIST OF FIGURES (continued) Page

NOMENCLATURE

A	constant
A'	constant
A_1	accelerometer
a	value of lead compensator zero
a',b	equivalent motor pole locations after application of first rate feedback loop
$B_{\#}$	voltage in control circuits
e	applied voltage to motor
f	flip flop voltage
FET	field effect transistor
G_D	lateral control system wave shaping network
G_J	longitudinal control system wave shaping network
i	motor current
J	polar moment of inertia
K	torque per unit current generated by motor or gain constant in transfer functions
K_4	back emf constant
K_{P_1}	gain of position feedback loop
K_{R_2}	gain of second rate feedback loop
$\overline{K}$	load gradient, torque per unit deflection
$\overline{K}/J$	ratio of load gradient to rotational inertia
P	pole location on s-plane
P_1	potentiometer
R	sum of R_a & $\frac{1}{2}R_F$
R_a	armature resistance
R_F	field resistance

R/C	rate of climb
SA	summing amplifier
T	generated torque
T_1, T_2	tachometer
T_L	load torque
V_f	forward speed
x,y,z	control voltages
Z	zero location on s-plane
δ	motor-voltage-killer-circuit voltage
λ	voltage in braking circuit
θ	motor shaft angle
$\dot{\theta}$	motor shaft velocity
$\ddot{\theta}$	motor shaft acceleration
ϕ_c	bank angle command
τ	time constant

STATEMENT OF PROBLEM

Design an electromechanical actuator for the aerodynamic surface depicted below:

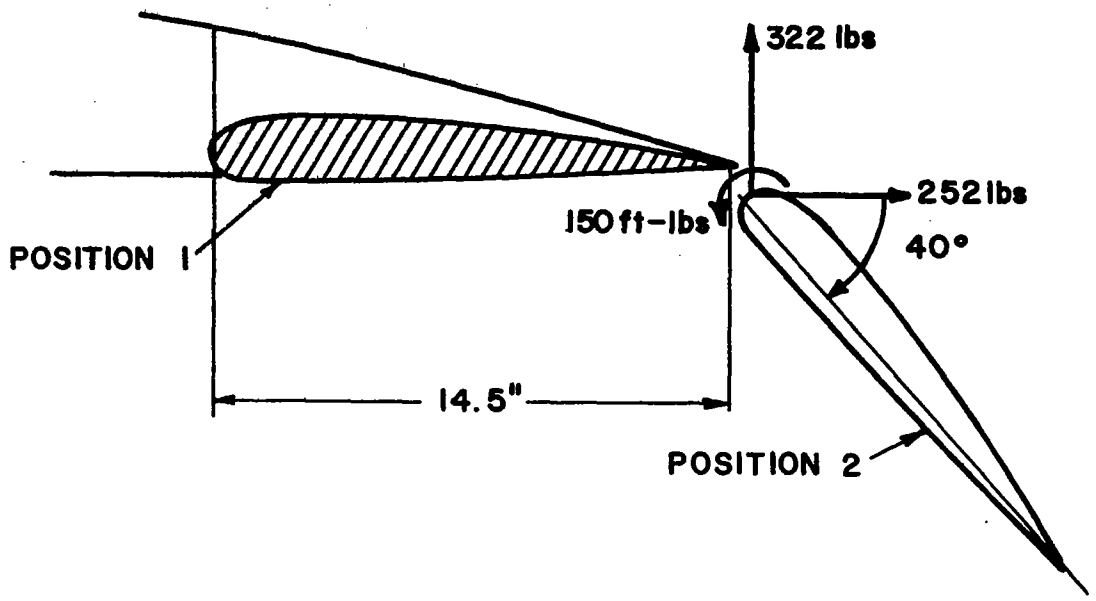

Note that in moving from position 1 to position 2 the surface moves rearward 14.5" while rotating 40°. The loads shown are the maximum encountered. They occur at half the maximum speed. It may be assumed that the aerodynamic loads vary linearly with displacement and as speed squared.

The surface weighs 45 lbs. The maximum displacement required as a function of speed is shown below:

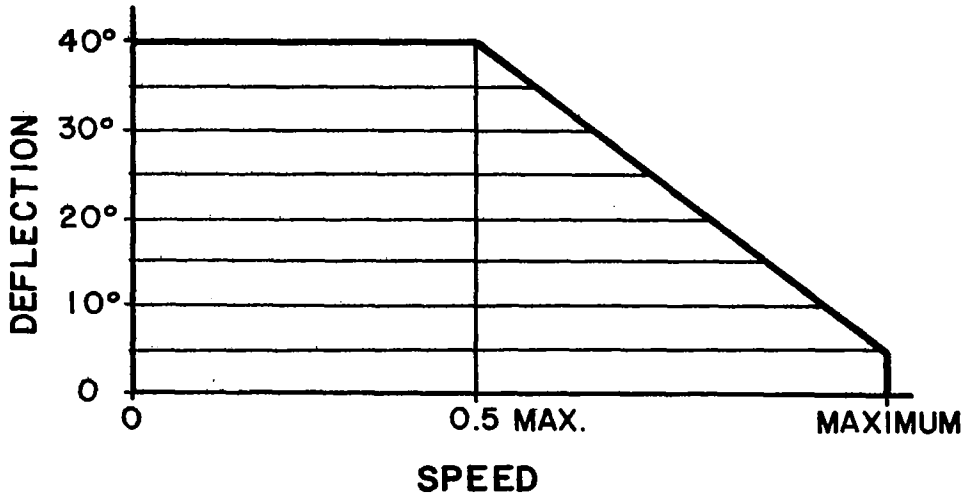

The surface will be excited by two command modes. The desired time histories of the surface may be represented as follows

MODE I

(WORST CASE AT 0.5 MAXIMUM SPEED)

— MOVE TO NEW POSITION AND HOLD

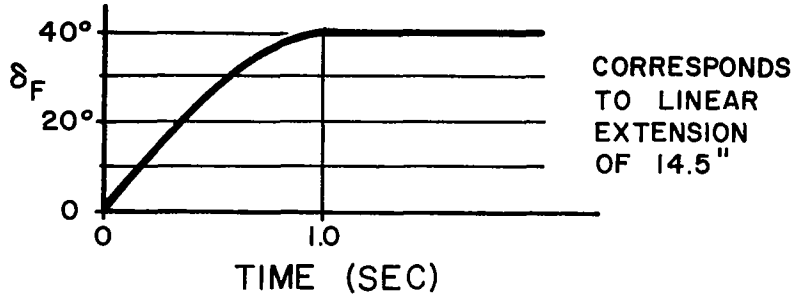

ASSUMED TRANSFER FUNCTION: $\frac{40°/sec}{s^2}$ FOR $t \leq 1.0$ sec.

MODE II

(WORST CASE AT 0.5 MAXIMUM SPEED)

— MOMENTARY DEFLECTION ABOUT EQUILIBRIUM POSITION

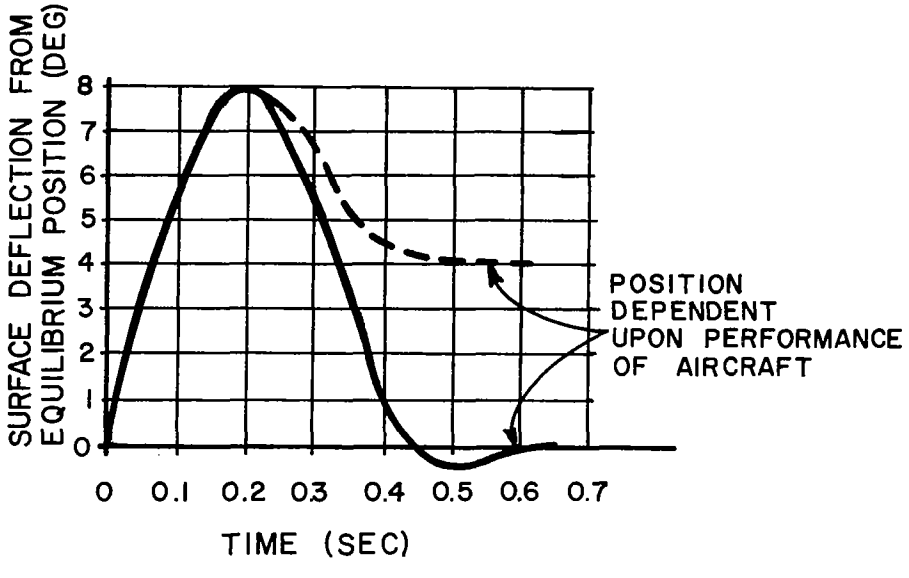

ASSUMED TRANSFER FUNCTION:

$$\frac{13.3°(2.3273)(S+20)}{S(S+12.8+9.6j)(S+12.8-9.6j)} \cdot \frac{40.2(S+2.74)}{(S+11)(S+30)}$$

It is desired that the surface follow these excitations with a first order lag not exceeding 0.02 seconds, that is, the transfer function of the actuator should be capable of being represented with reasonable accuracy by

$$\frac{A}{S + 50} \cdot \qquad A = 50\left(\frac{40 \text{ degrees}}{\text{system voltage}}\right) \cdot$$

Positioning accuracy of ±0.1° is desired for all surface deflections and airspeeds.

Excitation is to be removed from the actuator when the holding time exceeds 4.0 seconds. The surface must not move more than 0.1° when excitation is removed.

The actuator must be capable of operating from battery power in emergencies with unimpaired effectiveness. Battery drain is to be a minimum (< 2000 watts at any time).

No mechanical relays are to be employed.

Minimum signal-to-noise ratio at any nodal point in the system is to be 6 db.

Since the design approach to be evolved should be useable on a variety of aircraft and aircraft types or even in non-aircraft applications where high speed response and relatively small motors are required, no detailed consideration need be given to the mechanical design of the flap itself. It will be sufficient to assume that a preliminary stress analysis has concluded that a flap of sufficient stiffness, strength, fatigue life, operating smoothness, and aerodynamic effectiveness can be built at a weight of 45 lbs. It may be noted that despite the relatively speedy flap motion desired, inertial actuation loads on the flap are less than 22 lbs.

BACKGROUND

Direct lift control (DLC), stability augmentation and gust alleviation methods for aircraft are becoming more sophisticated with each passing year. An essential feature of any such system is a fast-acting, servo-driven aerodynamic control surface. These surfaces apply aerodynamic forces and moments to the aircraft at rates and amplitudes far beyond the capability of the human pilot while maintaining precise phase and amplitude relationships with the airframe motions.

Surface actuation is usually accomplished hydraulically. This is because

(1) in these situations the surface is rotated the required 25° or so by applying a large force to a short horn extending from the torque tube to which the control surface structure is attached. A hydraulic cylinder is ideally suited to applying a large force over a short stroke. Further, through the use of rapidly opening and closing valves (often electrically-operated) the full system hydraulic pressure is applied to the piston face almost instantaneously.

(2) oil pumps with pressure-relieving bypasses provide a very efficient means of transforming power from the low-torque, high-speed characteristics of the engine or an electric motor to the high-torque, low-speed characteristics of the linear actuator. The motor driving the oil pump can be operated at its maximum power speed while the motion of the actuator piston is determined by the volumetric output of the pump at rated pressure and the piston area needed to apply the desired force. Since most oil pumps will deliver excess flow quantities at discharge pressures less than rated, actuator piston speed will increase somewhat at reduced loads. Speed variations with load can also be reduced by including a gas-pressurized fluid accumulator in the system.

With suitable valving, the response of a hydraulic actuator to a step increase in cylinder pressure is similar to that of a spring-damper system with a time constant of 0.02 seconds or less. Devices of this type are found in modern military aircraft.

In considering the application of stability augmentation and gust alleviation devices to small, single-engine aircraft, it became evident that one would also like to have this level of control surface responsiveness ($\tau \leq$ 0.02 seconds) for these aircraft. Further, to provide the degree of alleviation desired, surfaces of high aerodynamic effectiveness such as full-span, 30% chord Fowler flaps on the wings would be required. With a wing chord of 48" such a flap must extend rearward about 14.5" and rotate 40° for maximum effectiveness. To satisfy the requirements of the alleviation system being considered the flaps must be capable of moving from full retraction to full extension in 1.0 second and of extending 8° about an equilibrium position within 0.2 second and return within 0.4 second.

Maximum air loads occur when the flap is fully extended and the airspeed a maximum. It was calculated that for the intended application, the highest airspeed for which full flap extension would be required was 114 ft/sec. At higher speeds, the maximum calculated loads were less because the maximum required flap extension was less. The gradient--air load per unit flap extension--however increases as airspeed squared.

Since light aircraft do not normally have hydraulic systems, it was felt that a severe maintenance burden would be introduced by so equipping such aircraft. It was therefore decided to attempt to design an electrical flap actuator. It was also felt that it would be easier to provide individual element backup/redundancy with an electrical system and that the total system weight, including backup/redundancy elements, might be lighter than an equivalent mechanical means of extending a full span Fowler flap accurately to any desired position, with the required speed, and against all airloads encountered in flight. Electrically, the actuator should be capable of being modeled by the transfer function

$$\frac{\text{shaft position}}{\text{input voltage}} \simeq \frac{\text{GAIN}}{0.02S + 1} .$$

DESIGN PHILOSOPHY

Consider for a moment the forces and moments required to extend or retract and rotate a Fowler flap. For the situation under consideration a moment of 150 ft-lbs. is required to rotate the flap about its leading edge. An additional force of 252 lbs. is required to translate the flap against its chordwise force. Note that a hinge point 22.5" below the leading edge of the flap would permit a simple rotation to accomplish the required flap motion. The torque about such a hinge would be 323 ft-lbs.

It is evident therefore that aircraft electrical motors with their torque levels of 1 ft-lb. or less must be geared down by a factor of perhaps 600 to serve in this application. A simple calculation will show that it is questionable whether the flap could be rotated in the time required with a motor operating at 4,000 rpm. It was decided therefore that the flap extension and deflection should be controlled by two tracks with the tracks taking as much of the load as possible. The tracks would be mounted to the rear spar and remain fixed to reduce the motional inertia.

To reduce motor size and cost it was determined to seek to keep motor horsepower rating to no more than twice the maximum power required at any point during the flap deployment.

To insure long motor life, a design objective would be to remove voltage from the motor during periods when flap motion was not required. The flap may be required to remain in an extended position, however.

Simplified analyses indicated that some advantage could be gained in operating the motor in the off-on mode. The difficulty in obtaining precise positioning (flap positioning accuracy approaching 0.1° was desired), the difficulty in performing analyses of the system dynamics, and the higher electrical stresses involved with this mode led to the decision to design the system as a linear follower. Since motor characteristics are not linear at significantly lower than rated voltages and since system friction adversely affects positioning accuracy in linear systems, provisions to account for these effects were desired.

Operation from a grounded center tap 60 volt D.C. supply was desired. Such a voltage would permit the use of 28 volt D.C. motors capable of both flap extension and retraction without resort to double pole switches. It would also permit the operation of standard aircraft systems and would provide for biasing flexibility in the design of control circuits. Inclusion of relays and mechanical switching devices in the design was not desired on reliability grounds.

MECHANICAL DESIGN

By mounting the flap in tracks--Figure 1 depicts a possible layout--one can reduce the actuation loads to comparatively small values. Initial studies indicated that the maximum actuator load due to aerodynamic forces would be 92 lbs. A value of 100 lbs was therefore selected as a design maximum to account for static friction and calculation inaccuracies. This loading occurs at maximum flap deflection (40°) and a dynamic pressure of 15 lbs/ft^2.

During the take off run the dynamic pressure is much less and the required deflection only about 30°. At the maximum forward speed for the aircraft the dynamic pressure is 60 lbs/ft^2 but the required flap deflections do not exceed 5°. The absolute values of the actuator loads therefore vary substantially with flight conditions.

The load per unit flap deflection, however, varies even more widely. During take off, it is near zero. At a dynamic pressure of 15 lbs/ft^2 it is 2.5 lbs/° and at a dynamic pressure of 60 lbs/ft^2 it is 10 lbs/°. It may be noted that this combination of loads and load gradients present very severe electrical design problems as will become evident below.

The flap track arrangement shown in Figure 1 permits the actuation of the flap to be carried out along a straight line. Hence, by connecting the actuator rod to the flap structure with a ball joint the actuator may be mounted rigidly to the wing structure without incuring bending moments on the actuator rod.

Because of the long throw involved and the need (to be shown later) to keep motional inertia and static friction to an absolute minimum, an acme screw driven by a ball nut was used as the actuator rod. The lead desired, 1/2" per revolution, dictated the use of a 5/8" diameter screw, which is more than adequate to carry the axial loads involved.

Selection of the remainder of the nut-to-motor gear train entails matching

(1) the power required to displace the load with

(2) the torque-speed characteristics of the motor.

The maximum power required is easily estimated by assuming that a 100# force must be displaced through 14.5" in one second. This yields 0.22 hp. Typically, D.C. motors used on aircraft exhibit their peak power output at a speed of about 4,000 rpm. Their torque increases almost linearly as the speed is reduced, being about twice the 4,000 rpm value at stall. To permit the motor to accelerate to its maximum power speed, the motor torque required at any flap deflection must not exceed the half-stall value. The maximum actuator load of 100# must be transformed by the gearing to a torque acceptable to the motor. Gear inefficiencies and friction appear as increases in the torque required.

The smallest motor which is capable of deflecting the flap at the required rate must be geared so that it will develop its maximum power at maximum load. If the power peak occurs at 4125 rpm, the motor must develop 4 in-lbs of torque at this speed to obtain 0.25 hp. A nut operating on a screw with a 1/2" lead will require a minimum torque of about 8 in-lbs to enable the screw to exert 100# of force. The motor must therefore turn twice as fast as the nut and must make 58 revolutions in moving the flap from one stop to the other. To accomplish this the motor must run at an average speed of 3480 rpm. Very little time is therefore available for acceleration and deceleration.

Motor acceleration is determined by the ratio of the excess torque--available torque minus load torque--to the system moment of inertia as seen at the motor armature. The armature for this size and type of motor typically has a moment of inertia of 1 to 1.5 x 10^{-5} slug-ft^2. The flap mass was calculated to be 1.3 slugs. The effective moment of inertia of the flap mass at the motor was calculated to be

$$\frac{150}{(\text{Gear ratio})^2} \times 10^{-5} \text{ slug-ft}^2.$$

The 5/8" diameter, 1/2" lead screw has an effective gear ratio of 4. Thus the overall gear ratio is 8. The average excess torque is 2 in-lbs. Thus the average angular acceleration may be as great as 4,000 rad/sec^2. Acceleration time is thus about 0.1 sec. Deceleration time would be similar. The average speed would therefore be 3700 rpm.

This is, of course, a very idealized calculation. The inertia of the gear train was not included and the minimum value of the armature inertia was assumed. Also, the average excess torque available is less than the arithmetic mean between the stall torque minus the load torque and zero excess torque near maximum power speed. This is because the motor spends more time near maximum power speed, where there is little excess torque, than near stall. These considerations lead one to conclude that a more powerful motor probably must be used.

A motor of twice the torque (and power) would require a gear ratio of 4 and only 29 revolutions to deflect the flap fully. the average speed required is then only 1740 rpm. The average angular acceleration calculated on the same basis as before is only about 3400 rad/sec^2 because of the greater reflected inertia. The average speed is about 1850 rpm greater than required, a margin which permits the use of voltage feedback, operation as a linear follower with a first order lag, and the use of finite inertias in the gear set. A 1/2 hp split series field D.C. motor was therefore chosen as the basis for further design. An overall gear ratio of 5 was selected to allow for gear and track friction losses and to reduce the reflected inertia somewhat. A spur gear with a diameter slightly larger than the ball nut is to be attached to the ball nut. The diameter was minimized to reduce gear set inertia. An idler gear provides the necessary spacing between the ball nut and the drive gear on the motor shaft. The pitch diameter of the gear on the motor shaft is 83% of the pitch diameter of the gear on the ball nut.

A second but light-weight gear is also driven from the motor gear. Having 3.5 times the diameter of the motor gear, it operates the shaft position, shaft velocity, and shaft acceleration* sensors which serve the feedback circuits.

Figure 2 shows a possible layout of the mechanical elements of the drive system. Also indicated on the figure are an overrunning clutch and brake attached to the ball nut and a solenoid for disengaging the main drive motor and engaging a low power backup. A discussion of the later system is beyond the scope of the present work. The overrunning clutch and brake provide the capability of removing power from the motor while the flap is being held in position against the brake by aerodynamic forces. For extension, the clutch overruns and the brake release solenoid is not activated. For retraction, the brake is released and the clutch housing rotates. The motional inertia is thus a minimum when the motor is working against a load and somewhat higher when the load tends to help drive the motor. While complex, this clutch-brake arrangement was found to offer both lower inertia and lower frictional torques than irrevisible worm-worm gear sets.

* A design for such a sensor is given in Appendix I.

ELECTRICAL DESIGN

Analytical Representation of Motor and Load

The manufacturer's torque-speed and torque-current curves for the motor selected are shown in Figure 3 for 28 volt input. Motor characteristics at lower supply voltages were not available. These data were linearized and the results are shown, along with resistance and inertial data in Figure 4. For purposes of analysis it was assumed that

(1) at any given motor speed torque varies linearly with voltage

(2) for a fixed voltage torque varies inversely with speed in a linear fashion

(3) current varies linearly with torque

(4) RL time constants are sufficiently small to be considered zero

(5) the load gradient for any airspeed is constant with flap deflection

(6) windage and bearing losses in the motor are zero

(7) winding resistance during operation was constant at a value between the no current value and the stall current value.

The motor-load combination is then represented by the equation

$$T - T_L = J\ddot{\theta} \tag{1}$$

where $\ddot{\theta}$ is the motor shaft acceleration

T is the generated torque

T_L is the load torque

and J is the moment of inertia.

But

$$T_L = \overline{K}\theta \tag{2}$$

$$T = Ki \tag{3}$$

and

$$e = K_4\dot{\theta} + Ri \quad \text{or} \quad i = \frac{e - k_4\dot{\theta}}{R} \tag{4}$$

where $\bar{K}$ is the load gradient

K is the motor torque constant

i is the motor current (it flows through both field and armature in this design since it is a split-field series motor)

K_4 is the back emf constant

R is the sum of the armature resistance and half the field resistance.

By substituting equations (2), (3), and (4) into (1), one obtains

$$K\,\frac{e - K_4\dot{\theta}}{R} - \bar{K}\theta = J\ddot{\theta}$$

or

$$\frac{K}{R}e = J\ddot{\theta} + \frac{KK_4}{R}\dot{\theta} + \bar{K}\theta \qquad (5)$$

In the Laplace domain this becomes

$$\frac{\theta(s)}{e(s)} = \frac{K/RJ}{S^2 + \frac{KK_4}{RJ}S + \frac{\bar{K}}{J}} \qquad (6)$$

The mechanical design in which this motor* is used will affect only the values of $\bar{K}$ and J. Note, however, that increases in system inertia reduce both the transfer function gain and its damping and are thus much more significant than increases in static friction which affects only the value of $\bar{K}$.

For the gearing selected and aerodynamic loading encountered, the value of $\bar{K}$ will vary from zero to about .015 ft-lbs/radian. The full 220 radian motor shaft displacement is required up to a $\bar{K}$ of .00375. For higher values, the product of $\bar{K}$ and the maximum displacement required is approximately constant. Total system inertia as seen by the armature for this gearing was calculated to be 8.8×10^{-5} ft-lb-sec^2. $\bar{K}/J$ for the system therefore varies from zero to 168. With the other parameter values from Figure 4,

---

* By itself the motor is represented by the transfer function $\frac{\theta}{e} = \frac{2100}{S(S + 70.2)}$

$$\frac{\theta}{e} = \frac{726}{S^2 + 24.2\ S + \overline{K}/J} \qquad (7)$$

gives the numerical values for the transfer function of the motor-load combination.

System Deficiencies

θ_{max} = 220 radians and e_{max} = 28 volts. Thus, the steady-state gain must be 7.857 for $\overline{K}/J$ of 42 or less. To achieve this, the motor gain may be reduced or feedback employed to make the value of the positional term equal to 92. For $\overline{K}/J$ less than 42 the feedback must be increased accordingly or a limit switch plus shock absorber must be used to halt the flap at the end of the track. For $\overline{K}/J > 42$, a decrease in D.C. gain with load is acceptable, at least for Mode I operation: motion from one equilibrium position to another. Whether it is also acceptable for Mode II operation--a pulse about an equilibrium position--must be determined by calculation.

It will be noted, however, that if constant positional feedback is employed--say $(50/726)\theta$-- then the value of the positional term for $\overline{K}/J > 94$ is sufficient to cause the system to oscillate. The condition may be corrected with rate feedback, a value of $(6/726)\dot{\theta}$ being required.

Examination of the poles of the transfer function with these amounts of feedback reveals that for all except the very highest loads, one of the two poles lies on or near the origin. Since a motor response resembling

$$\frac{\theta}{e} = \frac{A}{S + 50}$$

was desired, the system dynamics with this type of feedback would be clearly unsatisfactory. As a minimum, it would be necessary to move both roots to the neighborhood of -50 on the S-plane while keeping the gain for $\overline{K}/J < 42 \approx 7.857$.

In order to move the roots to the left and still preserve the D.C. gain, it is necessary to increase the forward loop gain of the system. One may not simply amplify the input signal to achieve this; the steady state voltage into the motor would then reach 28 volts for flap deflection commands much less than 40°. One can, however, take advantage of the fact that in Mode II operation the flap is never commanded to move more than about 8° from equilibrium. In Mode I operation, where the full deflection might be commanded, the voltage input rate will not exceed 28 volts/sec. Thus, if one were to amplify only the transient portions of the signal while maintaining the same D.C. gain, the desired result would be achieved.

The following sections detail the means by which this was accomplished as well as other steps which were taken to bring the motor characteristics to the required dynamic condition and D.C. gain for all expected values of $\overline{K}/J$.

First Loop

To insure that the motor will not oscillate as the load is varied, a small amount of rate feedback from T_1 is employed as shown in Figure 5. The gain value finally chosen, 5.8/726, was found to produce the most linear movement of the innermost pole with variations in $\overline{K}/J$.

The use of this rate loop permits the motor to be represented by the transfer function

$$\frac{\theta}{e} = \frac{726}{(S^2 + 30\ S + \overline{K}/J)}$$

This may be compared with the transfer function with no feedback given by equation (7).

Forward Compensator

A lead circuit of the type

$$\frac{5(S + a)}{S + (5a + 0.1)},$$

placed ahead of the motor as represented by

$$\frac{726}{(S + a')(S + b)},$$

has the effect of speeding up the system dynamics without altering the D.C. values. A gain of 5 was chosen to take advantage of the fact that in Mode II operation the maximum flap deflection command value is 8° from equilibrium (1/5 of a maximum 40°) while in Mode I operation the input transients are sufficiently slow that this increased high frequency gain will not be utilized.

To make this type of dynamic enhancement effective, it is necessary that the compensator zero have substantially the same value as the innermost pole for all values of $\overline{K}/J$. Figure 6 shows the required value of "a'" as a function of $\overline{K}/J$ along with an analytical representation of this variation. The latter was used as the basis for further analysis and to design the circuit to produce "a", given the values of $\overline{K}/J$. Discussion of the means by which $\overline{K}/J$ is measured is deferred until later.

With this forward compensator the motor is now represented by the transfer function

$$\frac{3630(S + a)}{[S + (5a + .1)][S + a'][S + b]}$$

Adaptive, Gain-Scheduled, Rate and Position Feed-Back Loops

With a motor gain of 3630, the feedback should be so adjusted that the value of the positional term formed by the two effective poles* is 460. The D.C. gain then has the required value of 7.857. This value must be maintained for $\overline{K}/J < 42$. For $\overline{K}/J > 42$ the value of the positional term may increase monatomically such that at $\overline{K}/J = 168$ it is no more than 1840. The rate term should be such that the system is near oscillation in order that both roots be as far to the left as possible. With the positional term equal to 460, the roots can be located around -20 and -23 on the S-plane.

It will be observed, however, that even if the compensator zero always negates the innermost pole, the remaining roots will still move appreciably with changes in load. Further, to employ feedback to hold the maximum flap extension to 40° despite these variations in load it is necessary to schedule the feedback gain according to a measurement of $\overline{K}/J$ or to apply so much feedback that the load variation will be imperceptible in comparison. Unfortunately, even with the forward compensator too much gain must be sacrificed to take the latter route. If the positional feedback gain must be scheduled according to the perceived values of $\overline{K}/J$ then so must the rate feedback gain in order to maintain both roots as far to the left on the S-plane as possible. For ease in mechanization, the feedback gain functions should be as simple as possible. After much trial and error, the positional feedback gain was successfully represented by three straight-line segments while the rate gain was represented by two straight-line segments. These functions are shown in Table I. A block diagram of the motor with these adaptive, gain scheduled elements is shown in Figure 7. The location of the three poles and of the zero for various values of $\overline{K}/J$ is given in Table II. Figure 8 shows the flap deflection possible with this feedback configuration as a function of airspeed.

Response Enhancement Loop

Although both roots are now always located to the left of -20 on the S-plane, the dynamic response of the flap to a deflection command is still slower than desired. Examination of Figure 9 which shows the motor input voltage and output response to a 5.6 volts step and 28 V/sec ramp reveals that the voltage on the motor does not stay near its maximum value very long. (Thus a linear means of keeping the voltage at a greater value would enhance the response.)

The means chosen to accomplish this task is to use positive acceleration and positive rate feedback. This has the effect of placing a zero between the two poles resulting from the feedback shown in Figure 7 and a second zero at the origin. Increasing the gain then drives the innermost pole to the outside zero and the outermost pole substantially to the left. A pole is added at -225 to reduce initial transients.

---

* The zero $(S + a)$ is assumed for the moment to cancel the pole $(S + a')$.

A reduction of the block diagram of Figure 8 is shown along with the positive feedback element in Figure 10. (The root locations for various loads are given in Table II.) In general there is now a root at about -22.5 and another at -32 or beyond. More positive feedback cannot be used without driving the system into oscillation.

Input Compensator

Although the system dynamics have been improved significantly with the aforementioned techniques and the required D.C. gain has been maintained, the system still does not resemble the desired

$$\frac{\theta}{e} = \frac{A}{S + 50}$$

As the final step in the process to achieve this goal, the input signal is modified in two stages. It first passes through a passive lead network,

$$\frac{S + 22.5}{S + 45} .$$

It is then bifurcated. In one branch it is simply amplified with a gain of 2. The other branch contains a rate-generating network with an operational amplifier as its principal element. The signals passing through two branches are then summed to form a free zero*. The net effect is to pass the input signal through the block diagram represented by

$$\left(\frac{S + 22.5}{S + 45}\right) \left(\frac{S + 35}{17.5}\right)$$

as shown in Figure 11. The input compensator serves to cancel the root which is always near -22.5 and replace it with one at -45. It also effectively reduces the order of the denominator while substantially canceling the pole near -35. The system therefore appears much like a simple first order system with a 0.022 sec. time constant. Figure 12 compares the response of this system with that of a simple first order to a typical command input. Little difference is noted.

Complete System

Figure 13a is a general block diagram showing all the elements of the system discussed thus far as well as the Mode I and Mode II signal shaping networks. Figure 13b is a legend for Figure 13a. Each of these shaping

---

* This device is employed outside feedback loops to avoid the consequences of imperfect pure rate generation which may be present in these circuits.

networks is fed in practice by a step-like signal. That selected as the worst-case input for Mode II is given by

$$\frac{9.33 \text{ volts } (12.8)(S + 20)}{S(S + 12.8 + 9.6j)(S + 12.8 - 9.6j)}$$

while that for Mode I is given by a 28 volt step. Figure 14 shows the system response (with the motor shaft displacement given in radians) and the motor input voltage for $\overline{K}/J = 0$, 42, and 168 for Mode I input. Results with a Mode II input are given in Figure 15. Figure 15 also shows the Mode II response and Motor Voltage when the flap is deflected 30° as a result of a Mode I input. Comparison of the results with the desired responses shows that the design goals have been met.

It may be noted that the system will accept input voltage rise rates of 80-100 volt/sec. The maximum expected in the service for which it was designed is only 37.4 volt/sec. Thus there is adequate margin to insure the system will not saturate and become non-linear. The system may also be used in applications requiring somewhat higher voltage rise rates.

Control Circuits

Also shown on Figure 13a are what may be termed control circuits, that is, circuits which control the operation of certain elements but which are not strictly part of the signal circuits, i.e., the forward loop and feedback circuits which shape the voltage driving the motor. There are four circuits of this type used in this system:

(1) the load sensor "a" generator, K_{R_2} generator, and K_{P_1} generator

(2) the brake release

(3) the motor voltage killer

(4) the static friction compensator

These will be discussed in order.

Rearrangement of equation (5) shows that

$$\frac{\overline{K}}{J} = \frac{1}{\theta}\left[\frac{K}{RJ}(e - K_4\dot{\theta}) - \ddot{\theta}\right] \tag{8}$$

Thus by measuring the input voltage, the shaft position, the shaft rate, and the shaft acceleration--the latter three quantities are also used as feedback voltage sources--and performing the operations indicated in equation (8) one has an instantaneous value of $\overline{K}/J$. Thus, even if the flap load gradient is not quite linear with deflection or some unusual load condition should evolve, the proper compensation and feedback gain is still generated.

The "a" generator merely operates on the $\overline{K}/J$ signal to produce the "a" control voltage used in the forward compensator. The K_{R_2} and K_p generators perform similar operations to provide the gain control voltages for the variable rate and positional feedback circuits which are the required functions of $\overline{K}/J$.

It was mentioned earlier that to retract the flap, the brake on the overrunning clutch must be released. The brake release circuit logic requires both a negative change in command voltage and a knowledge that the motor speed has reached zero before it calls for the brake to be released. The release command is amplified to drive the brake release solenoid. It has been assumed that the brake release solenoid has a time constant of 0.003 second or less. Compensation may be required to achieve this performance.

The positional feedback loop is provided with a special circuit which, after four seconds of no change in motor shaft position, switches electronically to a voltage equal to the command voltage, thereby driving the actual motor voltage to zero. Since the motor no longer develops sufficient torque to hold the flap in position, the aerodynamic loads drive the flap against the brake. The flap is thus held in position without requiring the motor to develop stall torque continuously during long periods in which no flap motion is required.

In order that the positional feedback may resume its function in controlling system dynamics when flap motion begins again, a means must be provided to switch out the steady or "motor killer" voltage when a command to move the flap is applied. Thus when a change--in either direction--is sensed in the voltage level after the forward compensator, the resulting pulse causes the steady positional voltage to be switched out and the circuit for which the dynamic analysis was performed to be reengaged.

There is no way in which a conventional follower can compensate for static friction in the mechanism. If, for example, a command were given to proceed to a certain shaft position the follower would move until the torque developed in the motor by the difference between the command voltage and the positional feedback voltage was too small to move the flap further against the static friction. This flap positioning error of course depends upon the level of static friction in the flap drive linkage but it is also affected by non-linearities in the motor characteristics near zero excitation voltage. Since very accurate positioning of the flap is required in this application, a special circuit to reduce this error was developed. Again, a branched signal path is employed. One path, which is always operational, has a gain of unity. The other has a gain of nine. The output from the two paths are summed. As long as a tachometer signal indicates that the motor is turning, the high gain path is not operational. If, however, there is a difference between command position and achieved position and there is no tachometer output indicating that motion has halted, both paths are operational and the signal is effectively amplified by a factor of ten. As soon as a substantial tachometer signal is generated, the high gain path is again switched out of the circuit. In this way the motor is pulsed to overcome friction and motor insensitivities.

The detailed functioning of these control circuits is discussed along with their possible realization in hardware in the next section.

POSSIBLE REALIZATION OF SIGNAL CIRCUITS

Circuits have been designed for realizing in hardware the signal and control functions discussed above. It should be emphasized at the outset that no particular effort was made to optimize the cost or number of components in these designs. Rather, the effort was intended to display one possible means of realizing the particular function in hardware. While the circuits are based on standard design practice, they have not as yet been constructed. Modifications may therefore be necessary.

Power Amplifier and Friction Compensator

All the signal circuits ideally should be relatively high impedence circuits. Thus, a power amplifier with unity voltage gain is required immediately ahead of the motor. Because the system is intended to be operable from a battery for short periods during engine-out conditions it is imperative that the power amplifier operate with minimum power drain. A schematic of the power amplifier evolved to perform the required task is shown in Figure 16. The power amplifier contains

(1) an oscillator

(2) a driver

(3) a power switch

(4) a smoothing capacitor

(5) a series voltage regulator

(6) an active network which generates a control voltage E_o^*

The oscillator consists of a flip-flop (transistors Q_3 and Q_4 which are being set and reset by the collector output of transistors Q_5 and Q_6). These transistors are in turn run by a differential amplifier (transistors Q_1 and Q_2) whose output is proportional to the difference between E_9' and E_o^* (see Figure 18). E_9' is the command voltage and E_o^* is the voltage drop across the series regulator. The oscillator output (taken from the collector of Q_4) is a 30 volt square wave with a fixed repetition rate. The width of the square wave is controlled by $E_9' - E_o^*$. If $|E_o^*| = 28$ volts and E_9' is zero, then ideally the oscillator output is a 30 volt pulse of zero duration repeated at a fixed rate. If $E_9' = 28$ volts the oscillator output is a steady 30-volt signal.

The function of the oscillator is to act as a control element for the power switch. This switch in essence allows energy to flow from the battery in pulses such that when these pulses are smoothed by the filter capacitor and the series regulator the amplifier output will be the same as E_9' but at an impedence approaching zero. Thus the switch is conductive for very short periods when E_9' is small but will be conductive continuously when $E_9' = 28$ volts.

The oscillator signal is amplified by the driver Q_7 so that sufficient current is available to operate the power switch, Q_8, which consists of four transistors in parallel. Four transistors are necessary to provide the 64 ampere motor stall current with an adequate margin of safety. The switch is operated by altering the base bias of Q_8.

As noted previously, the wave form produced by the power switch is a square wave. To reduce the motor electrical stresses and to permit a valid linear analysis to be made, this square wave must be converted to an equivalent D.C. signal. This is accomplished in two steps. First filter capacitor C_3 converts the pulse chain to a sine-like wave form. The series regulator then acts like a variable impedence. When the output voltage exceeds the desired value, the regulator impedence increases; when the output voltage is less than desired, the regulator impedence decreases. E_o* is the voltage drop across the regulator. This voltage is calculated by feeding the input and output voltages of the series regulator, E_{ISR} and E_{IO}, to the noninverting and inverting inputs of the summing amplifier SAI004 respectively. When this voltage drop decreases, E_o* is fed into the oscillator in such a fashion that the pulse width is increased and the regulator voltage drop increased.

The series regulator consists of

(1) a pre-regulator to prevent the ripple voltage from being amplified. (It consists of one break down diode DZ_2, one transistor Q_9, and two resistors R_{18} and R_{19}.)

(2) the series element (three transistors, Q_{10}, connected in a shunt common emitter configuration, each transistor having a current handling capacity of 30 amps)

(3) a beta multiplier

(4) a comparator element

(5) a sampling element

The Beta Multiplier is a transistorized element which boosts the output current of the comparator element to the level required to drive the base of the transistors of the Series Element. The Multiplier consists of seven (7) transistors; five (5) of these are identified as Q_{11} and are identical transistors connected in a common emitter parallel configuration. The base of these transistors is driven by the emitter current of transistor Q_{12} and its base is in turn driven by the emitter current of transistor Q_{13}. This last transistor is driven by the difference current between that of the collectors of Q_9 and Q_{14}.

The comparator element consists of transistor Q_{14} and it has a floating reference input voltage E_9' to its emitter. The base current comes from the sampling element. The operational requirement on this transistor is that it puts out enough collector current such that $I_{CQ_4} \geq I_{CQ_5} + I_{BQ_3}$. Capacitor C_4 has been added from collector to base to avoid high frequency instability.

The sampling element consists of two fixed resistors R_{20} and R_{21} and a wire wound potentiometer R_{sp}. The resultant series resistance must be such that 5ma flow into that branch. R_{sp_1} and R_{sp_2} (setting of the wire wound pot) are adjusted such that sufficient current flows into the base of the transistor under the worst case reference condition.*

The friction compensator, it will be recalled, is included to decrease the dead band behavior of the motor due to its internal friction. Figure 17 shows a schematic of this compensator. First diodes D_{9_E} and D_{9_R} allow passage of signal E9 into the extension and retraction channels respectively in accordance with the polarity of E_9. If E_9 is positive the extension channel is operational and the retraction channel is inoperational; if E_9 is negative the retraction channel is operational and the extension channel is unoperational. The friction compensator in both channels consists of identical circuits and hence it will be sufficient to describe the operation of only one of them. Consider the extension channel as depicted in Figure 17. The signal path is branched after diode D_{9_E}. One branch is passed through the noninverting connection of summing amplifier SA_{FC1} with a gain of one and the other branch is passed through summing amplifier SA_{FC2} with a gain of nine. The PNP, NPN, common collector, common base FET's arrangement (FET_{9_1} and FET_{9_2}) permit or inhibit passage of the signal through the high gain path. As long as a tachometer signal indicates that the motor is still turning one of the FET's acts as a short circuit and the signal does not pass through the high gain path. If, however, there is a difference between commanded and achieved position and there is no tachometer output--indicating that motion has halted--then both FET's bahave as open circuits and the signal passes through the high gain path. The output of amplifier SA_{FC2} is connected to the inverting input of amplifier SA_{FC1} with a gain of one. Thus with the last set of conditions the resultant signal E_{9_E}' is effectively equal to signal E9 amplified by a factor of ten. As soon as a substantial tachometer signal is generated, one of the FET's again behaves as a short circuit and the signal is again blocked from the high gain path and the resultant signal E_{9_E}' is equal to the signal E_9. In this way the motor is pulsed to overcome friction and motor insensitivities.

Scheduled Series Lead Compensator

Substituting the parameter values from Figure 4 into equation (8) one obtains

---

* The output of the voltage regulator is fed to the terminal of the split field series D.C. motor which makes it rotate CW. The motor-load combination is geared such that a CW shaft rotation causes extension of the flaps. The CCW input terminal of the motor is connected to the output of the voltage regulator of the Retraction Power Amplifier. This amplifier is identical to the Extension Power Amplifier described above except that is designed to operate with negative voltages and hence the supply connection is grounded. The parameter values for the Extension Power Amplifiers are listed in Table III.

$$\frac{\overline{K}}{J} = \frac{691.51}{E_\theta}\left[E_{10} - 3345 \times 10^{-5}\, E_\theta^{\cdot} - 144.6 \times 10^{-5}\, E_\theta^{\cdot\cdot}\right] \qquad (9)$$

Figure 18 shows the schematic of the circuit used to generate a voltage proportional to the instantaneous value of the load parameter $\overline{K}/J$ according to equation (9). Voltage signals from accelerometer A_1 and T_2 are fed through individual voltage dividers to the inverting input of summing amplifier SA200. E_{10}, the input voltage to the motor, is fed to the non-inverting input of SA200. The gain of each of these three channels is scaled so that the maximum value of the output due to each signal is ±10v. The output voltage of SA200 is fed to the z input of a BB4095/15 multiplier and the signal from potentiometer P_1 is fed to the X_1 input of the multiplier through a voltage divider which insures that the maximum value of this signal is ±10v. When the other multiplier terminals are connected as shown in the figure, the device performs division and its output is as indicated. Summing amplifier SA201 is required to invert the output of the multiplier and reestablish the proper voltage level.

The output of SA201, voltage $E_{\overline{K}/J}$, is used to generate voltages x, y, and z. Voltages x and y are equal to voltage $E_{\overline{K}/J}$ whereas voltage z is generated in the block labeled z generator. The schematic for this block is shown in conjunction with the scheduled lead compensator in Figure 19. Voltage z is used to adjust the zero and pole of this compensator. Voltages x and y control the variable gain of the position and rate feedback loops, respectively. The adjustments of the zero and pole of this lead network result in the cancelling of the motor pole nearest the origin and the addition of a pole at five times the original pole location.

Figure 19 shows the realization of this Scheduled Lead Compensator Network. In general the pole and zero of the transfer function of a lead network can be varied by varying the capacitance in its series branch or varying the resistances in the series and shunt branches. The latter approach is taken in this realization using transistors Q_A and Q_B to operate as variable impedances depending on their base voltages. These base voltages are generated by the network labeled "Nonlinear Function Generator" which yields voltage z as a function of voltage $E_{\overline{K}/J}$. It should be noted that a piece-wise linear approximation has been used to the nonlinear relationship between "a" and $\overline{K}/J$ shown in Figure 6. Three linear segments, each with a different slope, are emphasized. Voltage $E_{\overline{K}/J}$ which is proportional to the instantaneous value of $\overline{K}/J$ constitutes the input to the circuit. Its parameters are selected so that the desired segment slopes and break points are achieved.

By using identical transistors and feeding their bases with voltages z and z/4 respectively, the impedances in the series and shunt branches vary according to the variations of voltage $E_{\overline{K}/J}$ while always maintaining the desired four-to-one ratio of series to shunt impedance. In this fashion, and with capacitor C_1 maintained at a constant value, the variation of zero and pole of the network is obtained. When $E_{\overline{K}/J}$ is zero, both transistors are open circuits and the network consists of resistor R_3 in the shunt branch and capacitor C_1 in the series branch yielding the desired transfer function at this value of voltage. When $E_{\overline{K}/J}$ is not zero, the shunt impedance is effectively that of the parallel combination of R_3 and the impedance presented by R_2 and the variable impedance

of transistor Q_B. The purpose of summing amplifiers SA31 and SA32 is to provide the transient gain of five required. The parameter values are also summarized in Figure 19.

Gain Scheduled Rate Feedback Loop

As seen from Table II, the purpose of this loop is to feed back a variable rate signal the magnitude of which depends on the value of voltage Y. Figure 20 shows the schematic of the realization of this variable gain loop. The circuit consists of three main parts:

a) the variable gain generator
b) the multiplier and scaling networks
c) the switching voltages generator

The variable gain generator consists of three branches in parallel. The first branch, consisting of summing amplifier SA7 and FET_{70}, FET_{71}, and the associated resistances, generates the term [13 - .783Y] which is the required value of K_{R2} for $0 < Y < 8.93$ volts. The second branch, consisting of SA8 and FET_{72}, FET_{73}, and the associated resistances, generates the term [13.665 - .857Y] which is the required value of K_{R2} for $8.93 < Y < 14.3$ volts. The third branch, consisting of FET_{74}, FET_{75}, and a voltage divider network, generates the term [1.4] which is the required value of K_{R2} for $14.3 < Y < 30$ volts.

These branches are switched in and out of the circuit by means of electronic switches. Voltages B_1 and B_2 insure that FET_{70} and FET_{71} will be conducting when the FET's in the other two branches are not conducting; when B_1 becomes positive, FET_{70} and FET_{71} are not conducting and FET_{72} and FET_{73} are conducting. At the same time, B_2 insures that FET_{74} and FET_{75} are not conducting. Finally when B_2 becomes positive, FET_{74} and FET_{75} are conducting whereas the other FET's are not, the latter being accomplished by returning B_1 to a zero value when B_2 becomes positive. Note that FET_{70}, FET_{72} and FET_{74} serve as isolating switches.

The signal from the variable gain generator is fed directly to the X input of a multiplier, the Y input of which is connected to tachometer T_1 through a voltage divider network. The purpose of this voltage divider network is to insure that the maximum value of $E_{\dot{\theta}}$ is ±10 volts as is required by the multiplier. The output of the multiplier yields a voltage which is 3630/30 as large as the value of the desired voltage E_{R2}; hence amplifier SA9 and its associated resistances are introduced to perform the necessary scaling. The output of this amplifier--voltage $-E_{R2}$--is then fed to the inverting input of amplifier SA20.

The switching voltage generator produces voltages B_1 and B_2 which, as previously discussed, determine which of the three different gain branches feeds the multiplier. To generate B_1, voltage Y is compared with a fixed voltage of magnitude 8.93 volts in SA10; thus B_1 is negative for $Y < 8.93$ volts, zero for $Y = 8.93$ volts and positive for $Y > 8.93$ volts. To generate B_2, voltage Y is compared with a fixed voltage of magnitude 14.3 volts in SA11.

B_2 also goes through negative, zero, and positive values, depending on the value of Y with respect to 14.3 volts. Note that when B_2 becomes positive, B_1 becomes zero through the action of FET_{76}.

Gain Scheduled Position Feedback Loop

Table II also shows that the purpose of this loop is to feed back a variable position signal the amplitude of which depends on the value of voltage X. Figure 21 shows the schematic of the realization of this variable gain loop. The circuit consists of the following parts:

a) the variable gain generator
b) the multiplier and scaling network
c) the switching voltage generator

The variable gain generator consists of three branches in parallel. The first branch, consisting of summing amplifier SA12, FET_{78}, FET_{79}, and the associated resistances, generates the term [4.59 - .28X] which is the required value of K_{P_1} for $0 < X < 14.3$ volts. The second branch, consisting of SA13, FET_{80}, FET_{81}, and associated resistances, generates the term [1.39 - 0.56X] which is the required value of K_{P_1} for $14.3 < X < 17.85$ volts. The third branch, consisting of SA14, FET_{82}, FET_{83}, and the associated resistances, generates the term [.78 - .021X] which is the required value of K_{P_1} for $17.85 < X < 30$ volts. These branches are switched in and out of the circuit by means of electronic switching. Voltages B_2 and B_3 insure that FET_{78} and FET_{79} be conducting when the FET's in the other two branches are not conducting; when B_2 becomes positive, the second branch becomes operational and the first and third branches are out of the circuit; when B_3 becomes positive, the third branch becomes operational and the first and second branches are out of the circuit. Note that FET_{78}, FET_{80}, and FET_{82} serve as isolating switches.

The output from this multibranch network is fed directly to the X input of a multiplier the Y input of which is connected to potentiometer P_1 through a voltage divider network. The purpose of this network is to insure that the maximum value of E_θ is ±10 volts as is required by the multiplier. The output of the multiplier yields a voltage which is 3630/300 as big as the value of the desired voltage E_{P_1}; hence amplifier SA16 and its associated resistances are introduced to perform the necessary scaling.

The switching voltage generator is the part of the circuit which generates voltage B_3 which, together with voltage B_2, controls the presence of one of the three branches in the circuit. There is no need to generate voltage B_2 again since reference to Figure 18 will show that voltages X and Y are identical. Thus, voltage B_2, generated in the rate switching voltage generator network, is used in the switching of the position feedback loop. To generate B_3 voltage X is compared with a fixed voltage of magnitude 17.85 volts in SA15; thus B_3 is negative, zero, or positive depending on whether X is less than, equal to, or greater than 17.85 volts. Note that the connection of the output of amplifier SA11 (voltage B_2) in Figure 20 to the FET's in Figure 21 is electrically opened when B_3 becomes positive, since in effect B_2 becomes zero due to FET_{77}.

The output of SA16--voltage $-E_{P_1}$--is fed to the inverting input of SA20. This connection is controlled by FET_{84} which is activated by voltage δ. Also shown in the figure is a direct connection from potentiometer P_1 to the noninverting input of SA20. This connection is controlled by FET_{85} which is also activated by voltage δ. The purpose of this alternate unity gain position feedback is to relieve the motor of severe electrical stresses during long periods of constant flap position as already discussed. Note that both loops are not operational at the same time. The trigger signal δ is generated by the motor voltage killer circuit which will be discussed under realization of control circuits.

The combination of the feedback signals in SA20 is shown in Figure 22. The resultant signal is compared with signal E_5 in the summing amplifier SA3 as shown in Figure 23.

The subsystem can now be reduced by standard block diagram algebra to the block diagram shown in Figure 10 with the overall transfer function being as given by the equation

$$\frac{K}{(S + P_1)(S + P_2)} .$$

Improvement Feedback Loop and Fixed Compensator

The positive acceleration and rate feedback employed to improve the system response can be represented by the feedback element

$$H(S) = \frac{-70s\ (S + 22.5)}{3630\ (S + 225)}$$

and an external fixed compensator with transfer function

$$G_c(S) = \frac{(S + 35)(S + 22.5)}{17.5\ (S + 45)}$$

Figures 24 and 25 show the schematic realization of the improvement feedback loop and the fixed external compensator respectively. The output from the external compensator and the improvement feedback loop are combined in summing amplifier SA2 as shown in Figure 26. Note that the feedback is positive.

The final reduction of the block diagram can now be effected with the result as shown in Figure 27.

REALIZATION OF CONTROL CIRCUITS

For ease in fabrication, the friction compensator was included in the Power Amplifier design and the "a" signal generator was included in the Scheduled Lead compensator. These control circuits were discussed previously as part of the realization of the associated signal circuit elements. This leaves the motor voltage killer and the brake release circuit to be discussed at this time.

As mentioned previously, the motor voltage killer circuit generates a signal δ which opens and closes the electronic switches (FET's 84 and 85 in Figure 21) in the Gain Scheduled and Constant position feedback loops. These FET's control which loop is operational. Figure 28 shows the schematic of the realization of this circuit. Signal δ is the output of a Bistable asymmetrical flip-flop with inputs A and B which are generated as described below. The flip-flop has two states, which depend on the levels of A and B. *In state I, δ is high (+) and it makes the Gain Scheduled loop operational* while taking the constant gain loop out of the system. In state II, δ is low (-) and it makes the constant gain loop operational while taking the Gain Scheduled loop out of the system.

The flip-flop inputs A and B are functions of voltages E_7' and $E_{\dot{\theta}}$ respectively. Voltage A is generated in section (1) of the circuit whereas voltage B is generated in section (2) of the circuit. The flip-flop constitutes section (3) of the circuit. Section (1) consists of two identical rate networks through which E_7' is fed to the base of transistor $Q_7'_A$ and the emitter of $Q_7'_B$. The purpose of the transistors connected as shown in the figure is to provide the same signal output A whether the swing in E_7' is positive or negative. The parameters of the circuit are adjusted so that the output amplitude is enough to drive the set input of the flip-flop. Section (2) consists of a voltage divider network--R_{D1} and R_{D2}--to which the supply voltage is connected. This network gives the minimum voltage amplitude required to reset the flip-flop. The output of the network is switched electronically by FET's 86 and 87. These FET's are controlled by the rate voltage $E_{\dot{\theta}}$ in such a manner that there is conduction only when $E_{\dot{\theta}}$ is zero; for $\pm E_{\dot{\theta}}$ the output is grounded. The output of the voltage divider network feeds into an RC network with a one second time constant so that when the input is applied, it will take four seconds for the output to reach 97% of the input level. Thus four seconds after motion has halted a reset signal reaches the flip-flop. Section (3) depicts a standard flip-flop and will not be discussed.

The output of the flip-flop--voltage δ--is shown connected to the p-type FET_{84} and to the n-type FET_{85} of the Gain Scheduled and Constant position feedback loops to perform the electronic switching discussed above.

The brake release circuit controls the operation of the brake solenoid. Electrically, a deenergized solenoid causes the brake to be engaged and an energized solenoid causes the brake to be disengaged. These situations correspond to flap extension and retraction respectively. As shown in Figure 29, the power to the solenoid is controlled by a power FET which is opened

or closed by means of a logic circuit. The output of this circuit depends on whether a retraction or an extension command to the flaps has been given.

The earliest indication of the commanded flap motion comes from voltage E_3 (see Figure 13a). This voltage is fed into section (1) of the circuit through a rate network. The output of this network is fed to the base of transistor Q_{3A} which is simply functioning as an inverter. The collector and emitter of this transistor are connected to the set and reset input of a typical S-R flip-flop. These inputs are in effect the negation of each other. The resultant flip-flop output is f_1. A secondary indication of the desired flap motion comes from the output of the shaft mounted tachometer voltage $E_{\dot{\theta}}$ since when this voltage is zero it may indicate that a transition is about to take place. In section (2) of the circuit, this voltage is fed to the base of transistor Q_{3B} through diode D_o which is introduced to raise the on voltage of the transistor. Again the collector and emitter terminals of the transistor are connected to the set and reset inputs of a standard S-R flip-flop respectively. This flip-flop generates voltage f_2.

The requirement of the solenoid activation translates into the logical condition that both f_1 and f_2 must be at a high (+) level for the brake FET to conduct. This is achieved in section (3) of the circuit where a standard logical "and" gate has been shown schematically. The output of this gate is given by $\lambda = f_1 \cdot f_2$ which implies that voltage λ will be high (+) only where both f_1 and f_2 are high.

CONCLUDING REMARKS

The preceding sections have described the servo system devised to meet the requirements for an electrical actuator capable of moving a full-span, Fowler type wing flap very rapidly and very precisely over large excursions under all flight conditions which a typical light aircraft might encounter. A notable feature of the design is the use of an electrical motor with a power rating only twice the maximum power required. There is, in addition, a provision which removes electrical excitation from the motor when the flap position is stationary for periods in excess of four seconds, as well as a provision which serves to cover the effects of static friction and motor non-linearities at low excitation voltages. To achieve these capabilities circuits of some complexity were employed. These include a variable lead compensator in the forward loop, gain-scheduled rate and position feedback loops, a motor load sensor and various logic circuits. While it is not suggested that this particular design offers an optimum in performance to complexity ratio, it is presented in order to demonstrate the existence of at least one possible means of providing a level of aerodynamic surface response not achieved heretofore with electrical actuators.

The performance of the design has been evaluated by considering the components as ideal, lumped-parameter elements, amenable to linear analysis. In the absence of more detailed knowledge of frictional behavior, etc., a more elaborate analysis did not appear to be justified. A dynamically and kinematically accurate "boiler-plate" model, however, is now under construction and should be available to verify the predicted performance in late 1972.

APPENDIX I

ACCELEROMETER DESIGN

The design of the motor signal circuits calls for feeding back a signal proportional to motor shaft acceleration. Since differentiations are likely to induce noise and/or instabilities into feedback circuits, studies of possible direct-sensing accelerometer designs were also undertaken. Conventional angular accelerometer designs are not satisfactory because one must rotate the instrument housing through a possible 34 revolutions while maintaining noise-free electrical connections to the instrument interior. This would be difficult with slip rings or telemetry and coiling lead wires does not appear to be very practical. Also the rotational inertia of conventional designs is larger than desirable. The following design appears to overcome these objections.

Any direct-sensing angular accelerometer measures the torque needed to cause a known inertia to follow a rotational velocity. The torque is applied by a torsional spring of known spring constant. By measuring the displacement between the inertia and the shaft, one may then calculate the torque and hence the acceleration.

Suppose one mounts two equal diameter masses side-by-side on a shaft. The first mass is fixed, the second free to rotate. The second mass may be on a bearing to reduce frictional torque. It is connected to the shaft by a torsional spring. On the circumference of each mass are mounted one or more permanent magnet poles. The axis of the magnets are along the radii of the masses. Opposite the masses in the case of the instrument are small pickup coils. When the motor shaft turns, the magnets pass under these coils and induce a voltage pulse into them. Assume now that the coil opposite the fixed mass is connected to the set terminal of a flip-flop and the coil opposite the free mass is connected to the reset terminal of the flip-flop. Then the portion of any time interval during which the flip-flop is high is proportional to the lag between set and reset signals and hence to the shaft acceleration.

The spring constant and the mass of the free disc are so chosen that for the maximum acceleration expected the angular displacement of the free disc relative to the fixed disc is less than angular displacement between magnetic poles on the fixed disc. Thus the "on" time is always less than unity.

The device is pictured schematically in Figure 30.

APPENDIX II
EFFECT OF NOISE ON SYSTEM PERFORMANCE

As noted in Appendix I, a shaft acceleration signal is required in the feedback circuits. One possible means of generating it is to differentiate the shaft position indication twice. Assuming for the moment that this can be done perfectly, what is the effect of potentiometer noise on system performance? The study described below was employed to answer this question.

Assume that the potentiometer can be considered to generate sine waves of arbitrary frequency and amplitude as well as indications of shaft position. One can then derive the transfer function of system response to noise input. If the noise amplitude is taken to be a fixed percentage of maximum potentiometer voltage and if the system is linear, the effects of noise may be added to the response due to a command signal in order to obtain the total system response. Figure 31 presents output shaft amplitude as a function of noise amplitude and frequency. It will be seen that potentiometer noise is not a serious problem, even if it twice differentiated. No studies were carried out to determine the effects of imperfect differentiation, however.

The type of noise assumed here is analogous to that generated by a potentiometer wiper stepping from wire to wire. A more serious noise source, perhaps, is intermittant signal dropout due to dirt on the potentiometer windings. The equivalent sine wave amplitude is then equal to half the potentiometer voltage. The noise attenuation characteristics of the circuit, however, are such that the output shaft oscillation is within the positional tolerance specified. Note however that this analysis considers only the effects of noise in the positive feedback loop. It does not consider the effects of this noise in the other loops. In these loops the noise is fed back negatively with an appropriate attenuation.

One other aspect not included in this noise study is the electrical noise generated by components subjected to aircraft vibrations. In the absence of a knowledge of the specific components and their location in the aircraft, however, it is not feasible to develop a meaningful analysis.

APPENDIX III

ALTERNATE APPROACHES AND THEIR PROBLEMS

The complexity of the design discussed herein immediately seems to challenge those with long experience in the control field to find a simpler solution. Probably their first thought is to consider the system sketched below:

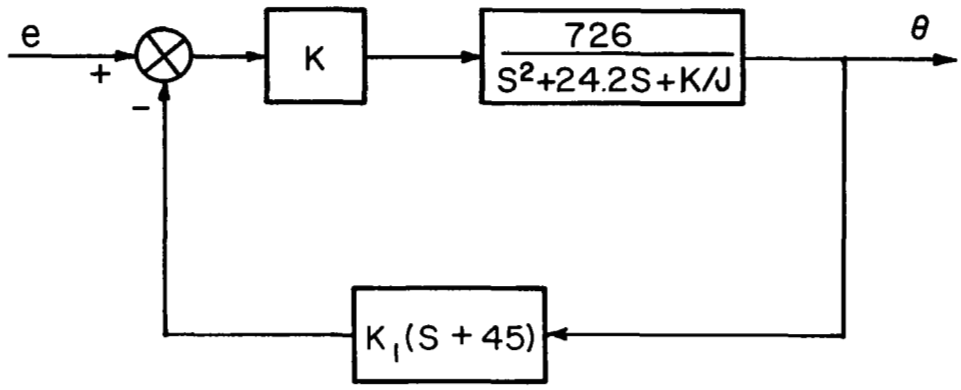

Its root locus with increasing K,

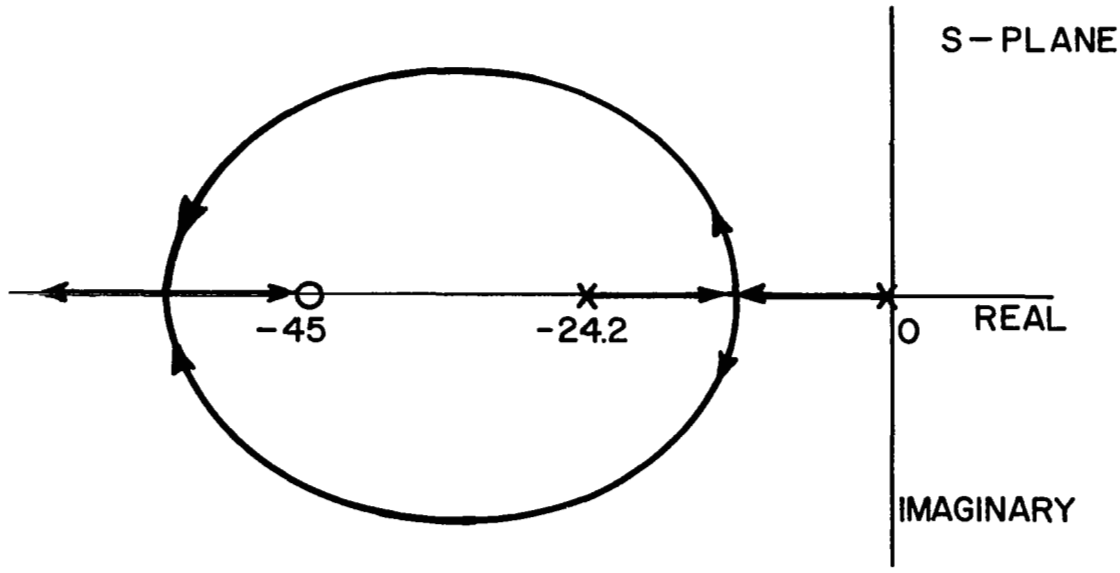

indicates that with a sufficiently large value of K one can drive the roots to positions on the real axis at about -45 and -225. The response characteristics

with this location are just those desired. To achieve this positioning of the roots,

$$\frac{\overline{K}}{J} + (726KK_1)\ (45) \simeq 10{,}000.$$

Since $\overline{K}/J$ varies only from zero to 168, one can readily see that variations in load hardly affect the position of the roots, also a desirable feature. The required value for KK_1 is then 1/3.27.

The required D.C. gain of 7.8 is achieved when

$$\frac{726\ K}{(726KK_1)(45)} \simeq 7.8$$

Hence, $K_1 = 1/351$ and $K \simeq 107$.

With these values, the maximum voltage at the amplifier input is about 0.27 volts. Examination of the error transfer function

$$\frac{\varepsilon}{e} = \frac{S^2 + 24.2S + \overline{K}/J}{S^2 + (24.2 + 222)S + \overline{K}/J + 10{,}125}$$

shows that for a rapid input the initial value of the error signal is about equal to e. Thus a command larger than .27 volts will drive K into saturation momentarily. In effect, this reduces the value of K and the roots move back along the locus. The error transfer function also shows that the D.C. value of ε/e is acceptably small for $\overline{K}/J < 8A$. For a large command value, say near 28 volts, the roots will be near 0 and -20 until the feedback begins to build up. They then leave the real axis, come together again and finally move to the desired locations. The response will therefore be very slow initially and then begin to oscillate. As the motion continues the oscillation subsides and the shaft rapidly goes to the command position. The time required to reach command position will probably be quite acceptable and the oscillation may not persist long enough to be troublesome. However, it requires a non-linear analysis to determine the response quantitatively. This requirement presents some problems in modeling the servo as an element in an otherwise linear control system. There is little value, however, in seeking alternate <u>linear</u> versions of the servo because it may be readily demonstrated that the present configuration or simple derivatives of it operated in a linear mode cannot simultaneously satisfy the requirements for (1) motor input voltage less than 28, (2) modeling by a first order time constant of 0.02 seconds, and (3) d.c. gain of 7.8. Hence, additional studies are needed to determine whether operation in the non-linear mode, perhaps with an altered configuration, would be advantageous. It is probable that a non-linear servo will be capable of shorter response times at the cost of increased electrical and mechanical stresses. Even though the number of components in a non-linear version can be expected to be substantially less than for the adaptive, gain-scheduled linear version discussed in the body of the report, the overall reliability will probably be less because of the higher stress levels.

$$K_{R_2} = \frac{1}{3630}(13.0 - 0.784\ Y) \qquad 0 < Y < 8.93$$

$$= \frac{1}{3630}(13.646 - 0.856\ Y) \qquad 8.93 < Y < 14.3$$

$$= \frac{1.4}{3630} \qquad Y > 14.3$$

In general $K_{R_2} = \frac{1}{3630}(A - B)$

$$K_{P_1} = \frac{1}{3630}(459 - 27.97\ X) \qquad 0 < X < 14.3$$

$$= \frac{1}{3630}(139.1 - 5.6\ X) \qquad 14.3 < X < 17.87$$

$$= \frac{1}{3630}(78 - 2.18\ X) \qquad X > 17.87$$

In general $K_{P_1} = \frac{1}{3630}(C - D)$

TABLE I. GAIN-SCHEDULED RATE AND POSITION FEEDBACK FUNCTIONS

$\frac{K}{J_T}$	MOTOR + LOAD + INNER RATE FEEDBACK			SCHEDULED LEAD COMPENSATOR			GAIN OF RATE AND POSITION FEEDBACK		REDUCED TRANSFER FUNCTION			REDUCED TRANSFER FUNCTION INCLUDING THE POSITIVE ACCELERATION FEEDBACK AND FORWARD LOOP COMPENSATOR							
	NUMERATOR	DENOMINATOR ROOTS		GAIN	ZERO	POLE	K_{R_2}	K_{P_1}	NUMERATOR	DENOMINATOR ROOTS		NUMERATOR GAIN	NUMERATOR ROOTS				DENOMINATOR ROOTS			
0	726	0	-30.00	5	0	- 0.10	13.00	459	3630	-23.10	-20.00	207.43	-22.50	-35.00	-225.0	-45.00	-22.25	-32.62	-143.23
5		- 0.17	-29.83		- 0.17	- 0.95	12.30	434		-22.83	-20.27						-22.38	-32.46	-143.25
10		- 0.34	-29.66		- 0.34	- 1.80	11.60	409		-22.60	-20.46						-22.48	-32.35	-143.25
20		- 0.69	-29.31		- 0.69	- 3.59	10.20	359		-21.97	-21.13						-22.61	-32.28	-143.23
30		- 1.04	-28.96		- 1.04	- 5.30	8.80	309		-22.56	-20.50						-22.63	-32.42	-143.16
42		- 1.47	-28.53		- 1.47	- 7.45	7.12	249		-22.86	-20.19						-22.47	-32.90	-143.03
50		- 1.77	-28.23		- 1.77	- 8.95	6.00	209		-23.70	-19.50						-22.27	-33.40	-142.90
60		- 2.16	-27.84		- 2.16	-10.90	4.47	159		-23.67	-19.54						-22.33	-33.54	-142.80
75		- 2.75	-27.25		- 2.75	-13.85	2.17	84		-24.20	-19.06						-22.12	-34.25	-142.59
84		- 3.17	-26.83		- 3.17	-15.65	1.40	55		-24.84	-19.40						-22.14	-35.62	-141.98
90		- 3.38	-26.62		- 3.38	-17.00		49		-24.78	-20.24						-22.31	-37.49	-141.08
100		- 3.82	-26.18		- 3.82	-19.10		39		-25.73	-20.95						-22.39	-40.80	-139.54
110		- 4.28	-25.52		- 4.28	-21.50		35.1		-25.74	-22.68						-22.79	-43.94	-137.89
120		- 4.76	-25.24		- 4.76	-23.14		31.2		-26.95	-22.83						-22.95	-47.56	-136.04
130		- 5.25	-24.75		- 5.25	-26.35		27.3		-29.35	-23.15						-22.93	-51.63	-133.96
140		- 5.78	-24.22		- 5.78	-29.00		23.4		-31.79	-22.83						-22.76	-56.17	-131.59
150		- 6.34	-23.66		- 6.34	-31.80		19.5		-34.46	-22.40						-22.49	-61.24	-128.83
160		- 7.00	-23.00		- 7.00	-35.10		15.6		-37.63	-21.87						-22.12	-66.97	-125.53
168		- 7.46	-22.54		- 7.46	-37.40		12.48		-39.90	-21.44						-21.75	-72.21	-122.29

TABLE II. SERVO TRANSFER FUNCTIONS

RESISTORS	KILOHMS	RESISTORS	KILOHMS	RESISTORS	KILOHMS
R_P	5.0	R_6	.5	R_{15}	1.00
R_0	1000.0	R_7	2.0	R_{16}	10.00
R_i	1000.0	R_8, R_9	10.0	R_{17}	.50
R_1	2.0	R_{10}, R_{11}	2.2	R_{18}	1.60
R_2, R_3	3.5	R_{12}	5.0	R_{19}	4.00
R_4	1.0	R_{13}	50.0 (5w)	R_{20}	.60
R_5	2.0	R_{14}	100.0 (2w)	R_{21}	2.70
				R_{P_o}	.50

TRANSISTORS	TYPE	CAPACITORS	µf	DIODES	TYPE
Q_1, Q_2, Q_3, Q_4	2N1304	C_p	.02	D_1	1N748
Q_5, Q_6	2N1305	C_2	.001		
Q_7	2N2905	C_3	10^3		
Q_8	2N5301	C_4	.01		
Q_9	2N2905				
Q_{10}	2N5301				
Q_{11}	TIP31				
Q_{12}	TIP29				
Q_{13}	2N696				
Q_{14}	2N338				

TABLE III. PARAMETER VALUES FOR THE EXTENSION POWER AMPLIFIER

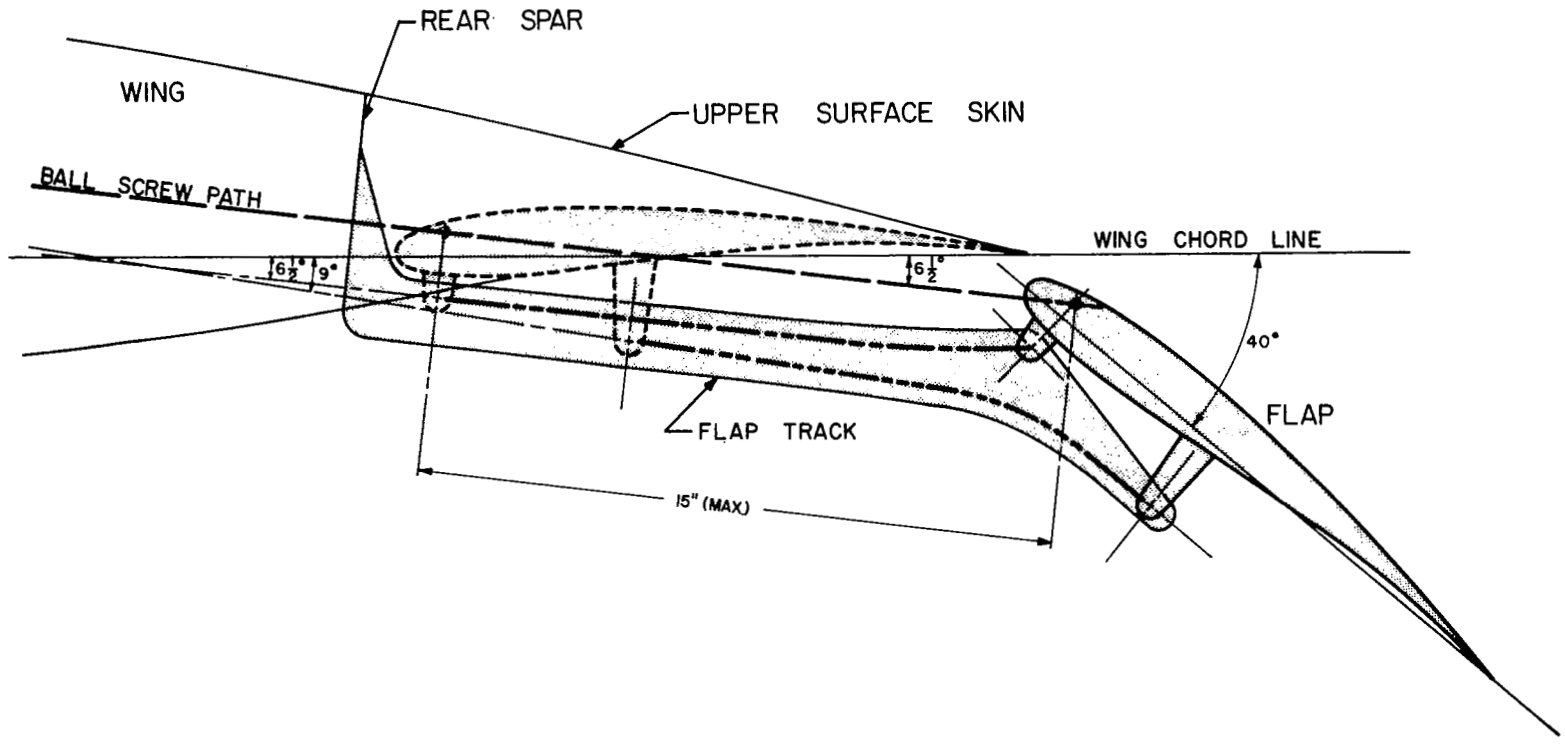

FIGURE I. FLAP TRACK AND ACTUATOR LAYOUT

① MAIN MOTOR
② SPLINE CONNECTOR
③ SOLID CONNECTOR
④ POTENTIOMETER
⑤ RIGHT ANGLE DRIVE
⑥ BACKUP SYSTEM SOLENOID (DASHED LINES)
⑦ TACHOMETER
⑧ BALL SCREW
⑨ BACKUP MOTOR
⑩ BRAKE SOLENOID

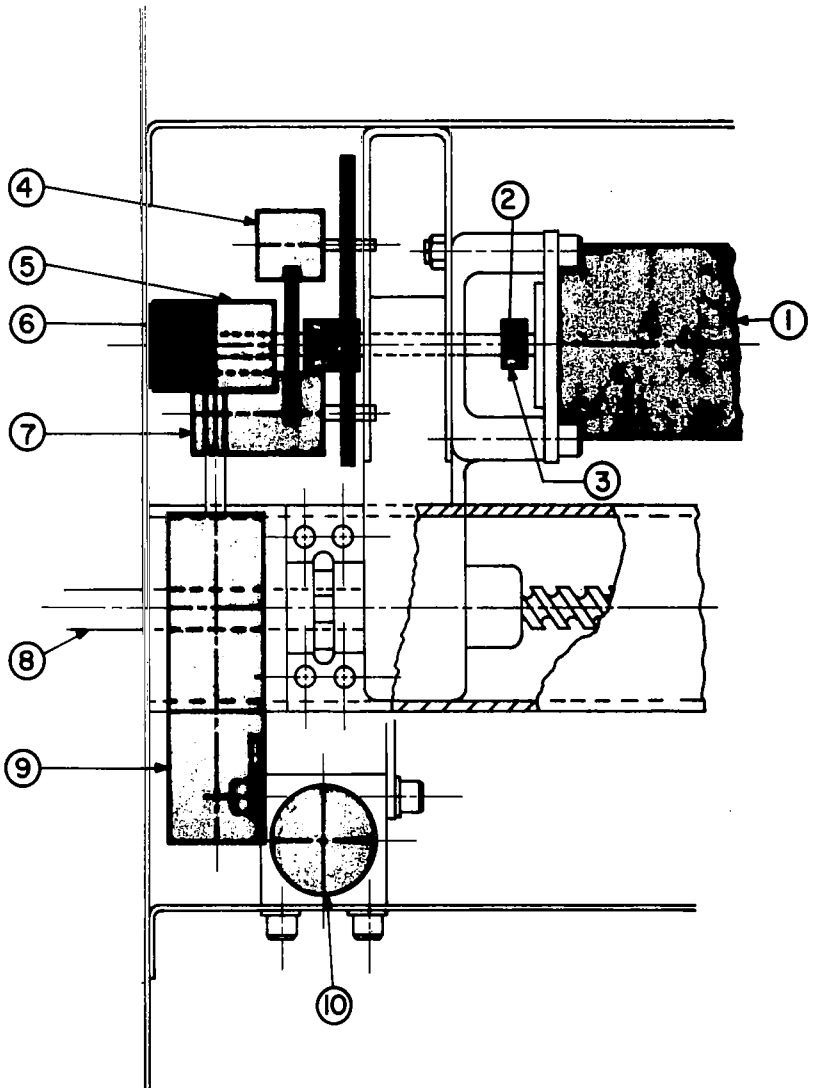

FIGURE 2. POSSIBLE LAYOUT OF MECHANICAL ELEMENTS

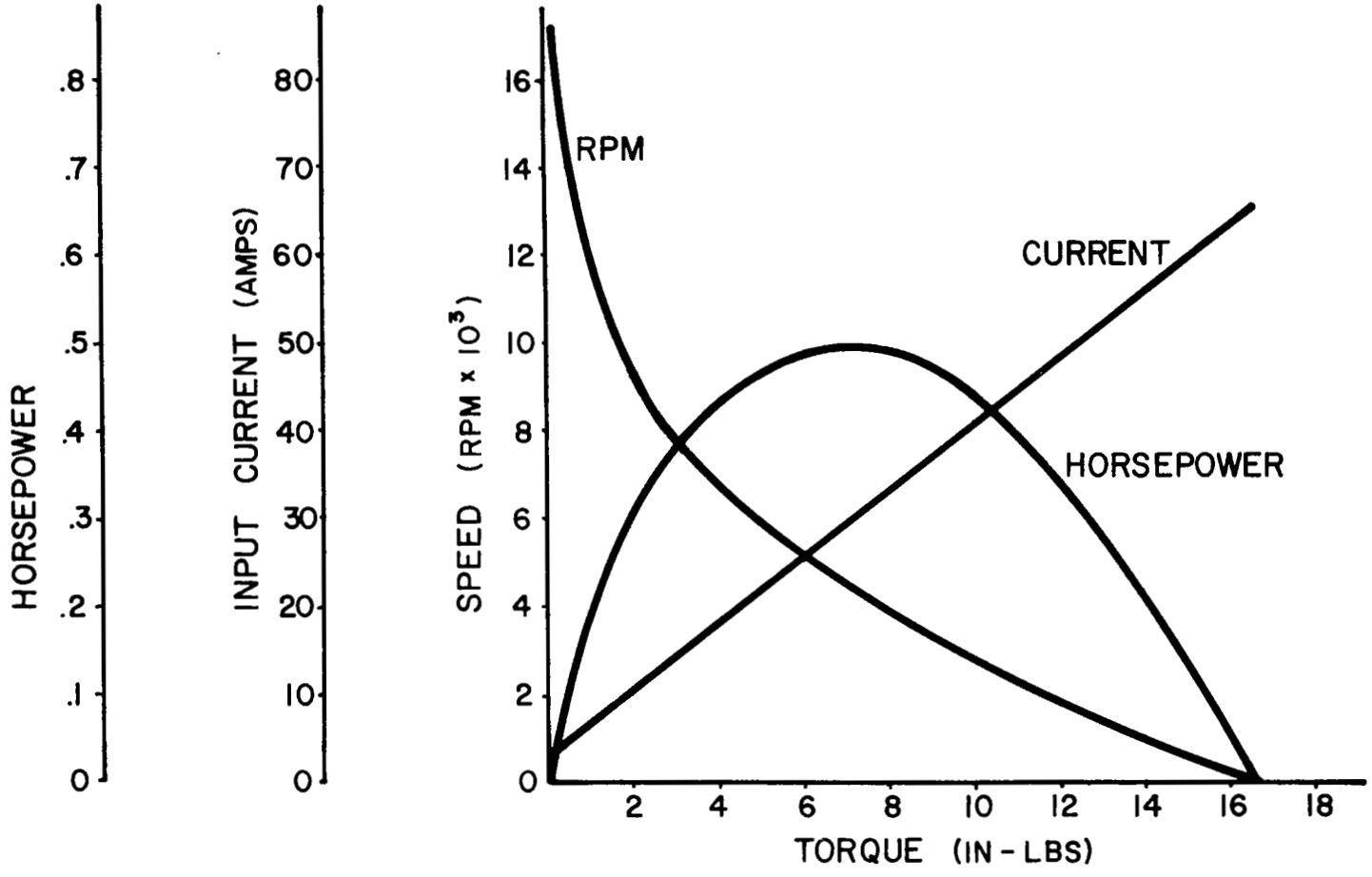

FIGURE 3. DC SPLIT SERIES MOTOR

SPERRY MOTOR 2940131 (SPLIT FIELD SERIES)

$J = 1.8\ \text{oz-in}^2 \times \frac{1}{16} \times \frac{1}{322} \times \frac{1}{144} = 2.426 \times 10^{-5}\ \text{ft-lb-sec}^2$

$K = 1.375\ \text{ft-lbs}/64\ \text{amps} = 0.02148\ \text{ft-lbs/amp}$

$R = 0.4375\ \text{volts/amp}$

$K_4 = 0.03345\ \text{volt-sec}$

$\bar{K}$ = variable

$e_{max} = 28\ \text{VDC}$

$i_{max} = 64\ \text{amps}$

FIGURE 4. ELECTRICAL AND INERTIAL CHARACTERISTICS

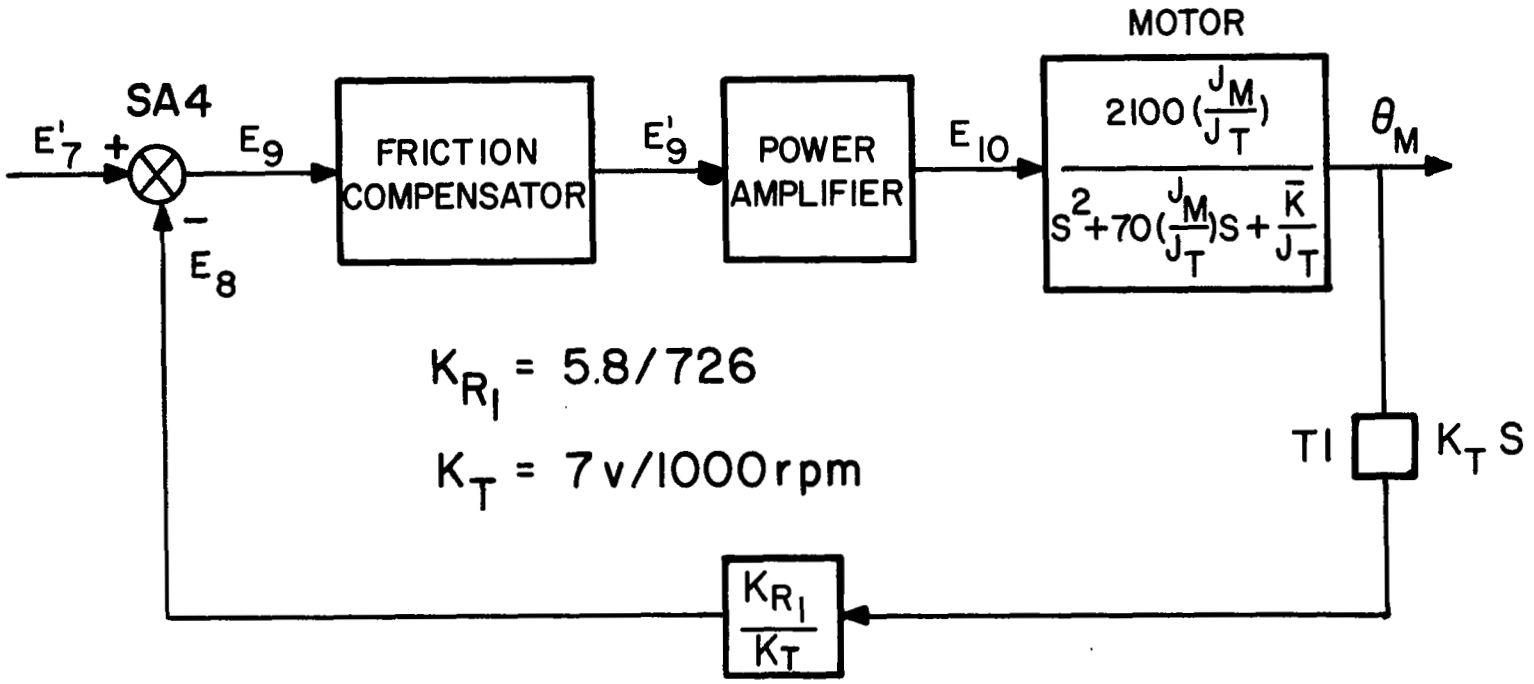

FIGURE 5. INNER RATE FEEDBACK LOOP

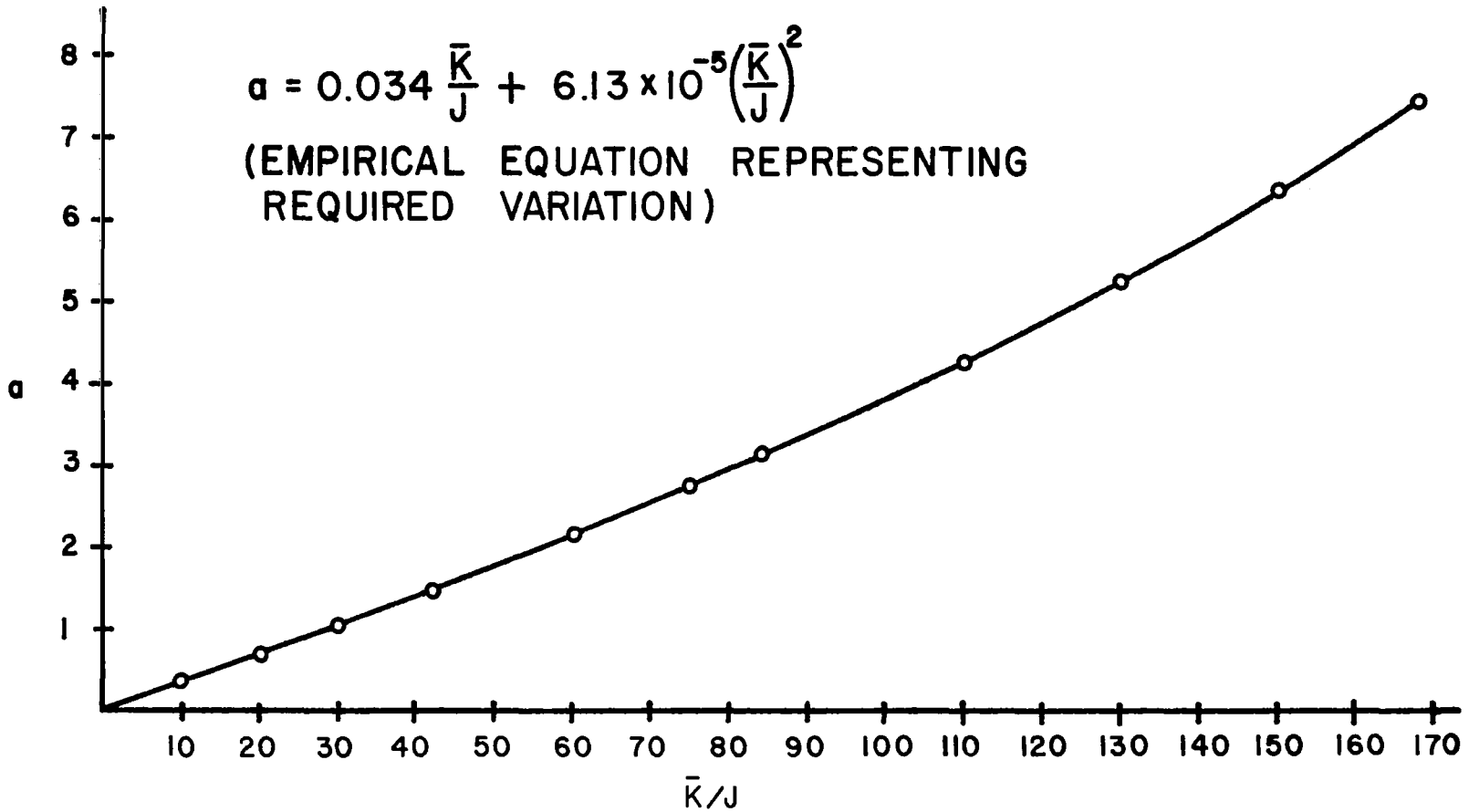

FIGURE 6. REQUIRED COMPENSATOR ZERO POSITION VARIATION WITH $\bar{K}/J$

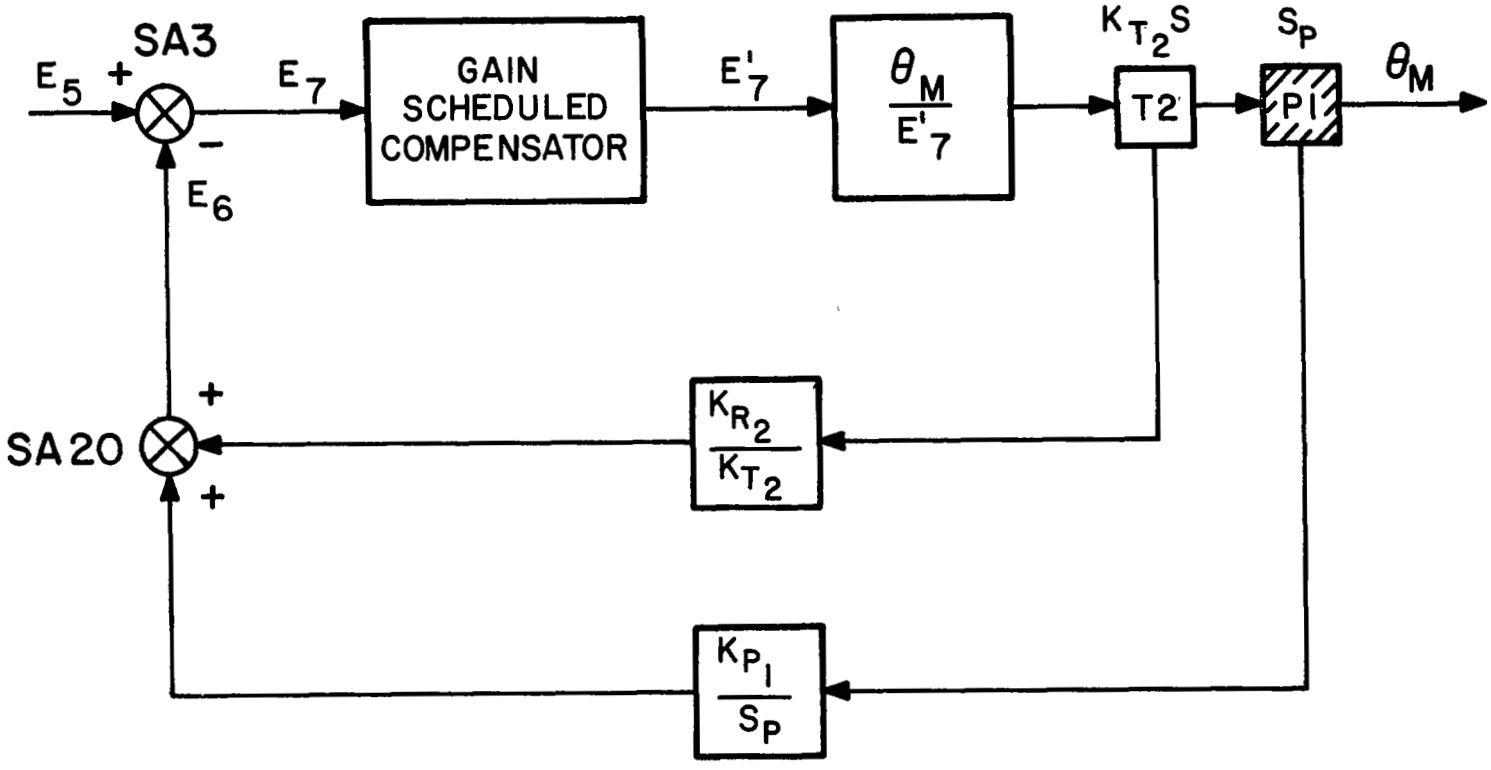

FIGURE 7. MOTOR WITH ADAPTIVE GAIN-SCHEDULED ELEMENTS

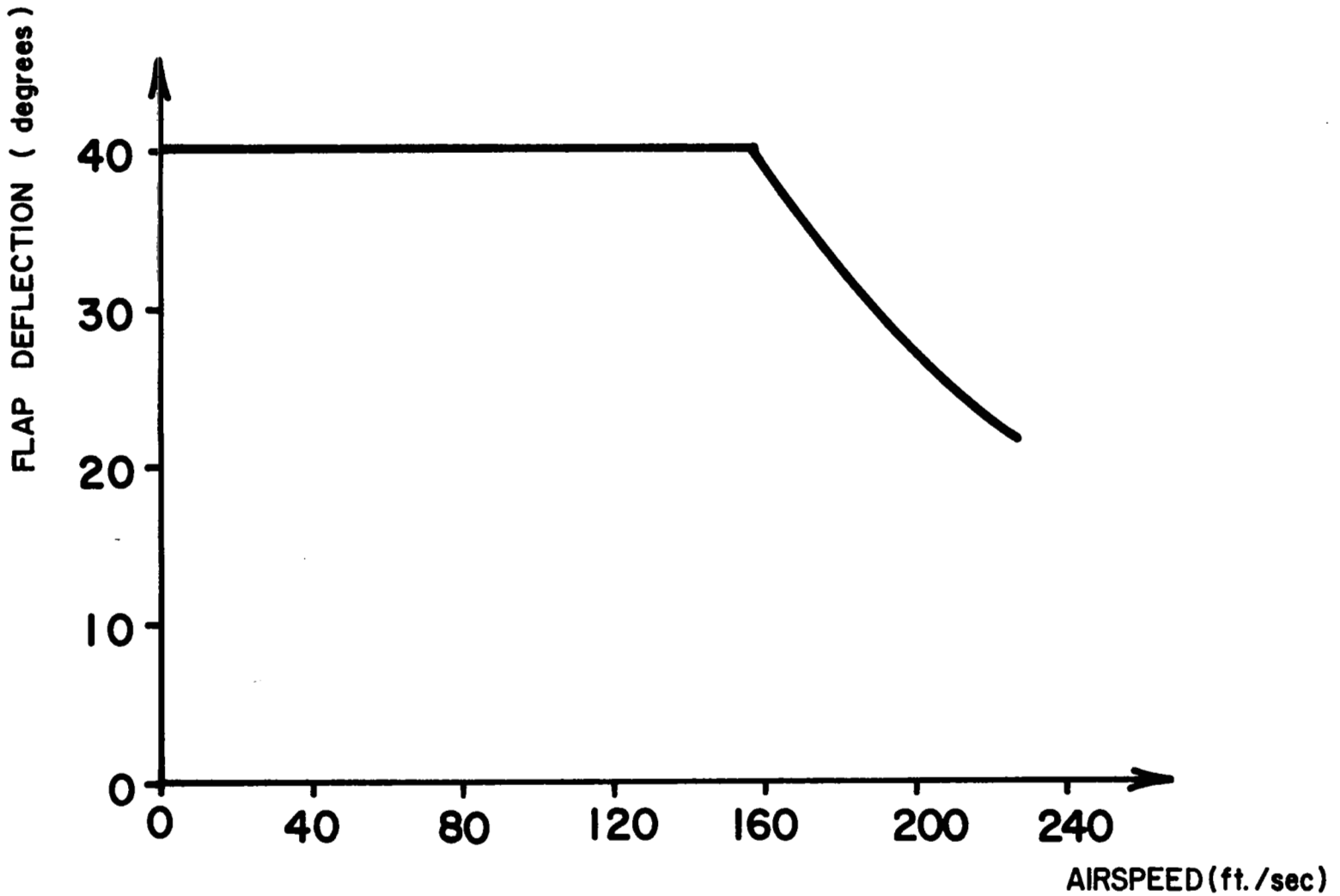

FIGURE 8. FLAP DEFLECTION CAPABILITY WITH SERVO SYSTEM

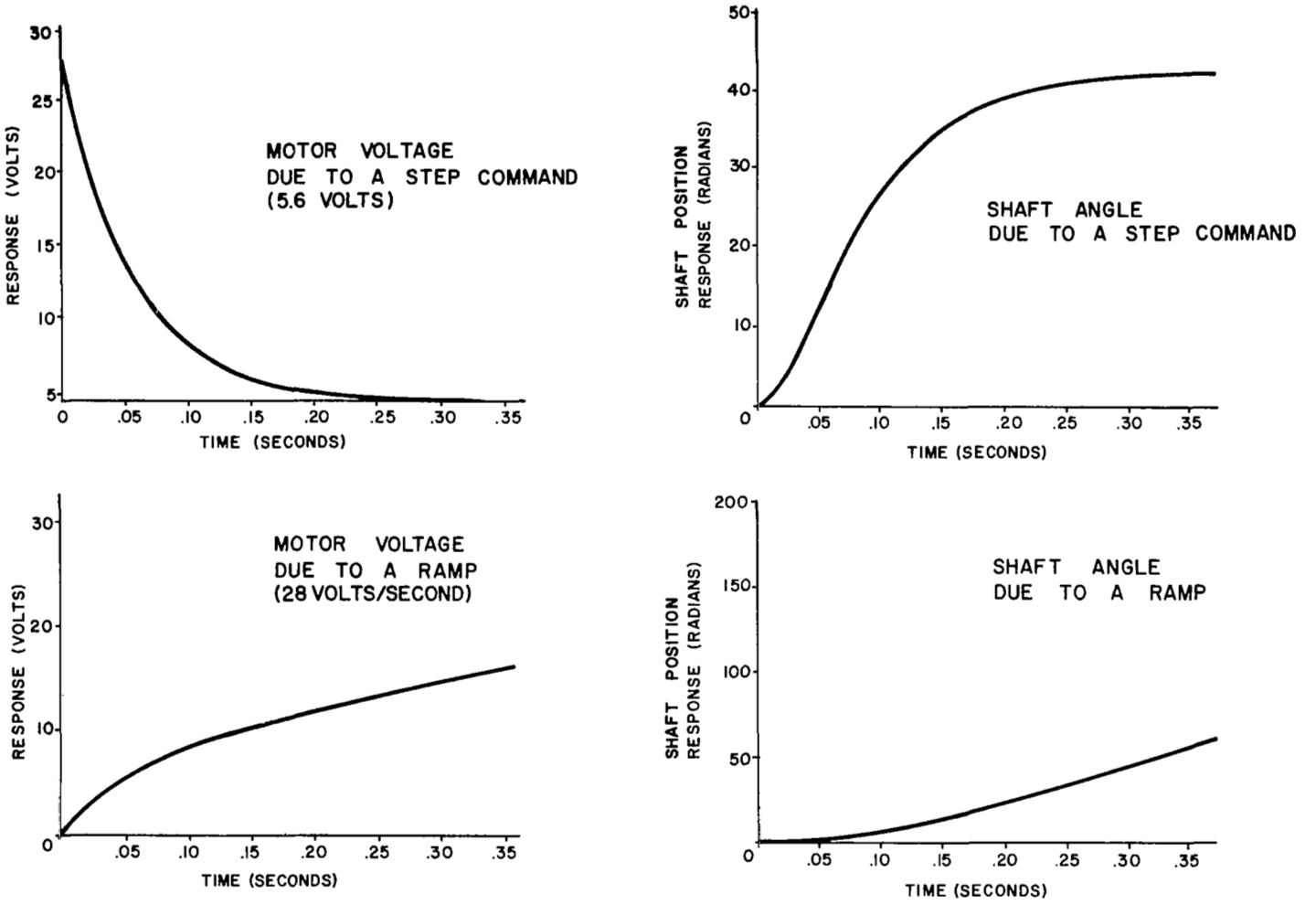

FIGURE 9. MOTOR VOLTAGE AND SHAFT ANGLE RESPONSE FOR SYSTEM WITH ADAPTIVE, GAIN-SCHEDULED ELEMENTS (NO POSITIVE FEEDBACK OR INPUT COMPENSATION)

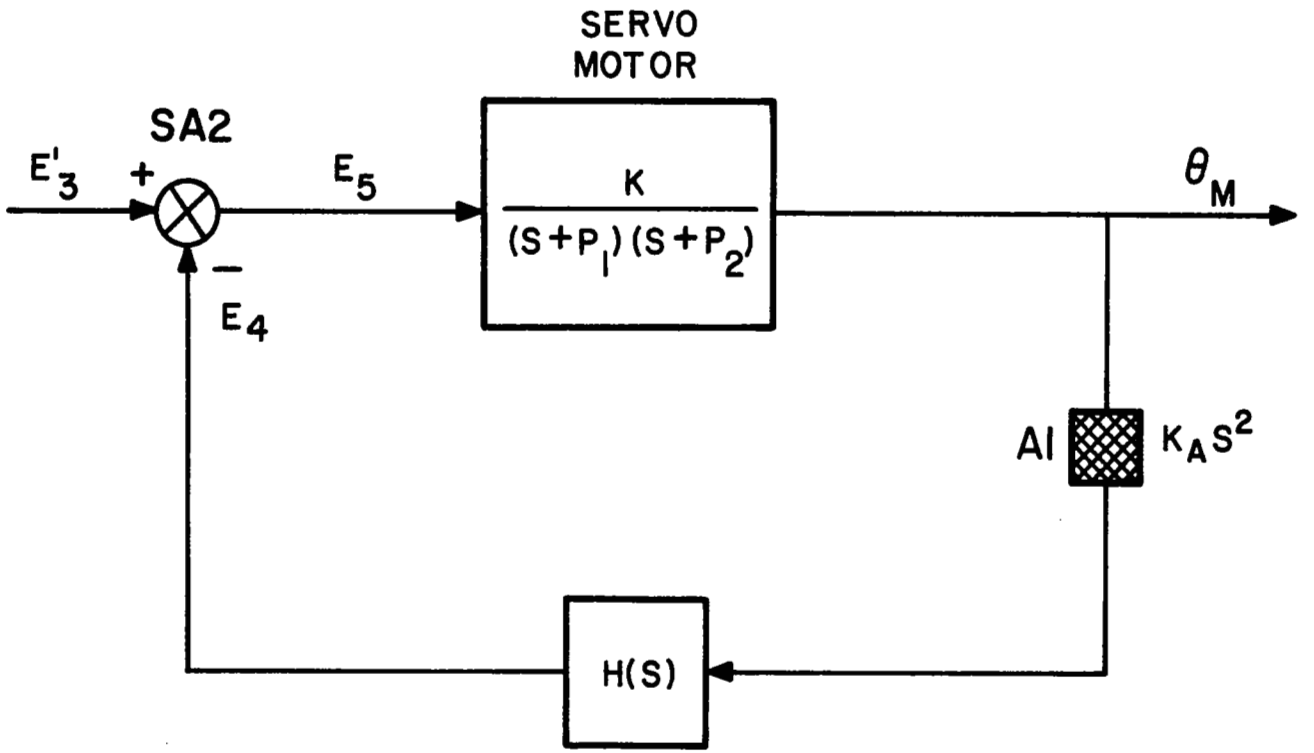

FIGURE 10. REDUCTION OF BLOCK DIAGRAM OF FIGURE 8 AND ADDITION OF POSITIVE FEEDBACK

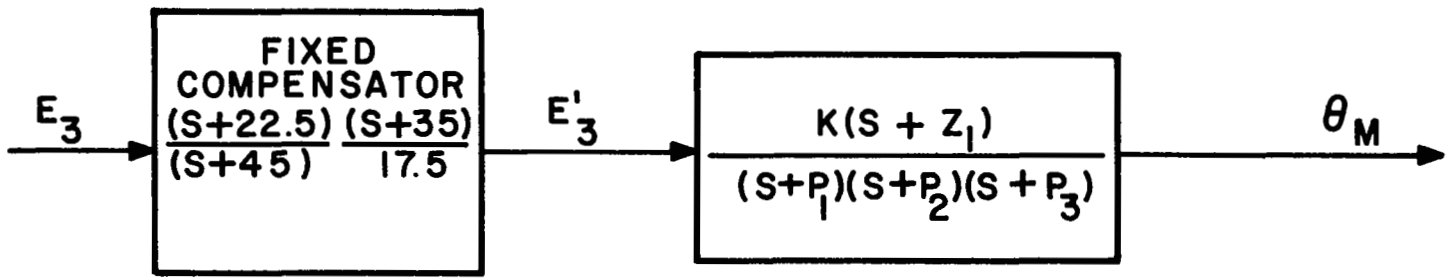

FIGURE 11. REDUCTION OF BLOCK DIAGRAM OF FIGURE 10 WITH FIXED INPUT COMPENSATOR

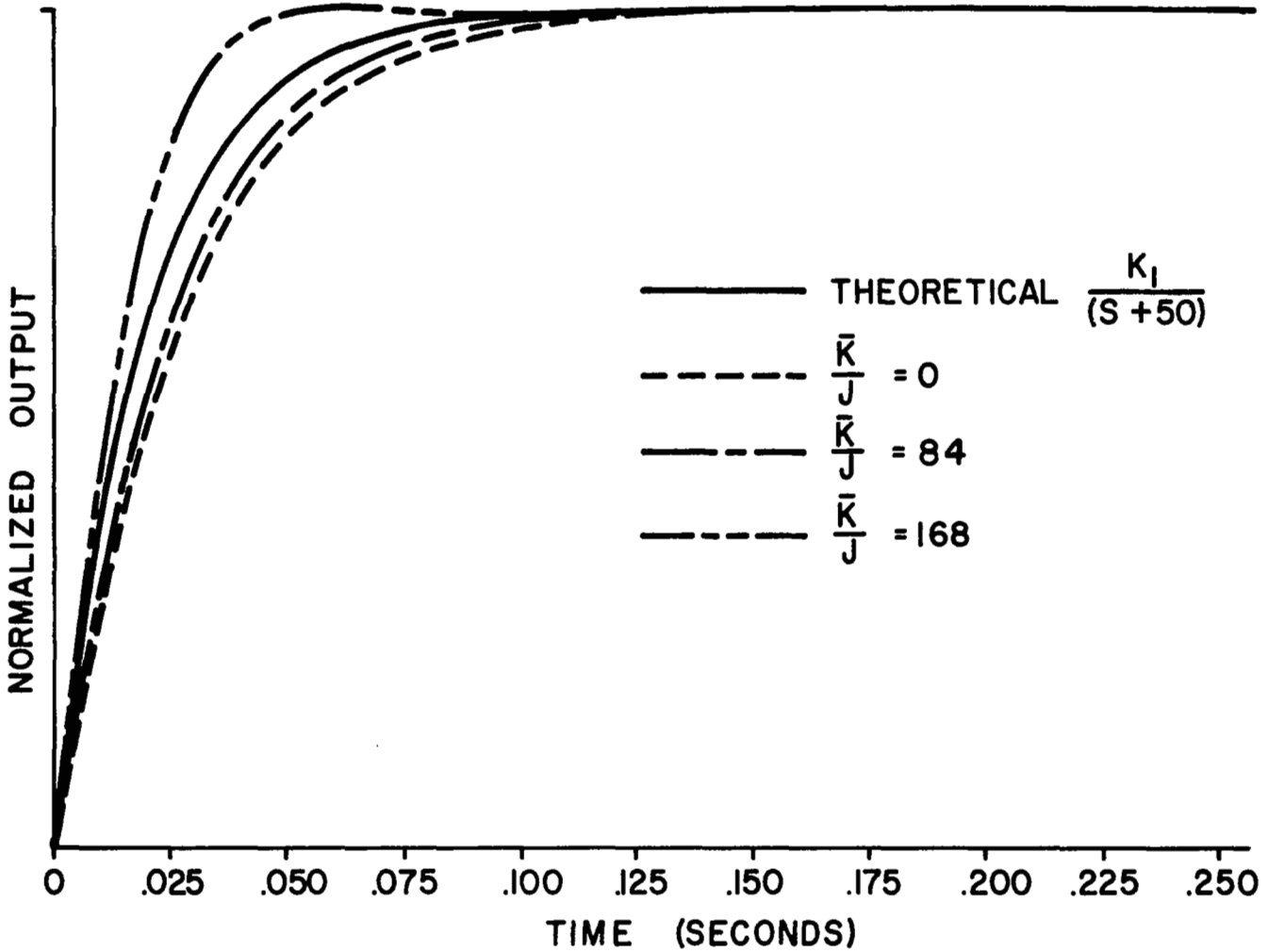

FIGURE 12. RESPONSE CHARACTERISTICS OF NCSU SERVO FOR VARIOUS $\bar{K}/J$'S VS. THEORETICAL

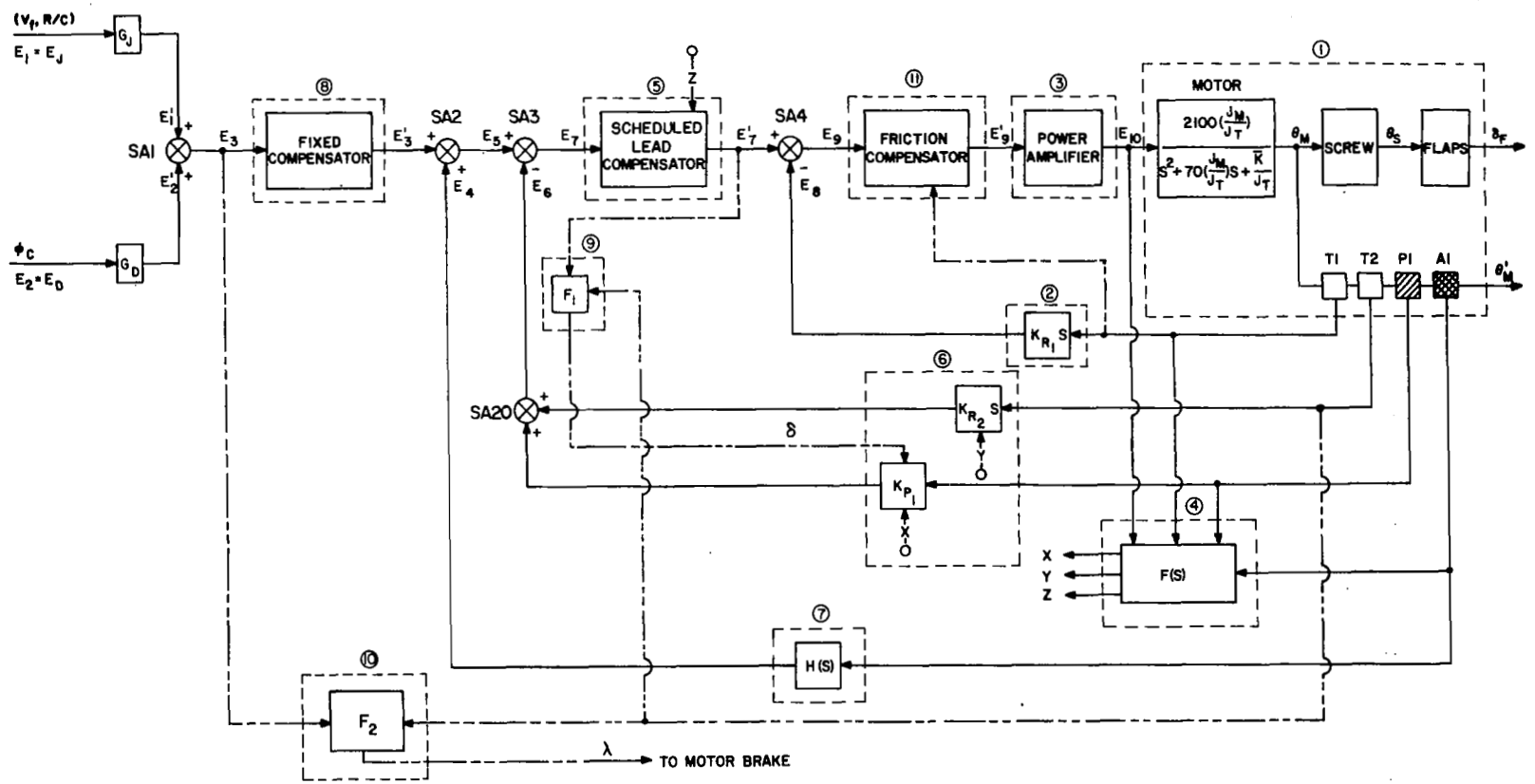

FIGURE 13a. BLOCK DIAGRAM OF FLAPERON SERVOACTUATOR

① MOTOR ACTUATOR-LOAD AND OUTPUT SENSORS

P1 TEN TURN POT. θ_M ; MOTOR SHAFT ANGULAR POSITION

T1, T2 TACHOMETERS θ'_M ; SENSOR SHAFT ANGULAR POSITION

A1 ACCELEROMETER θ_s ; LEAD SCREW ANGULAR POSITION

δ_F ; FLAP DEFLECTION

② FIXED GAIN NEGATIVE RATE FEEDBACK LOOP (FIGURE 5.)

③ POWER AMPLIFIER DRIVING THE MOTOR (FIGURE 16.)

④ GENERATION OF VOLTAGE PROPORTIONAL TO THE LOAD PARAMETER $\frac{R}{J}$ (FIGURE 18.)
(X, Y, Z ARE VOLTAGES PROPORTIONAL TO THE VALUE OF $\bar{R}/J$)

⑤ SCHEDULED LEAD COMPENSATOR (Z IS THE SCHEDULING PARAMETER) (FIGURE 19.)

⑥ GAIN SCHEDULED RATE ($K_{R2}S$) AND POSITION (K_{P1}) NEGATIVE FEEDBACK LOOP
(Y AND X ARE THE RESPECTIVE SCHEDULING PARAMETERS) (FIGURES 20, 21.)

⑦ RESPONSE ENHANCEMENT POSITIVE FEEDBACK LOOP (FIGURE 24.)

⑧ FIXED INPUT COMPENSATOR (FIGURE 25.)

⑨ MOTOR VOLTAGE KILLER CONTROL CIRCUIT (FIGURE 28.)

⑩ BRAKE RELEASE CONTROL CIRCUIT (FIGURE 29.)

⑪ STATIC FRICTION COMPENSATOR (FIGURE 17.)

E_J : FLAP ACTUATOR INPUT SIGNAL FOR MODE I OPERATION

G_J : MODE I COMMAND SHAPING NETWORK $G_J(s) = 1/s$. REALIZATION IS AS SHOWN :

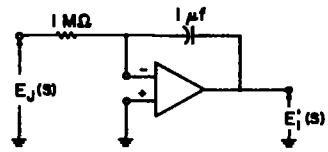

E_D : FLAP ACTUATOR INPUT SIGNAL FOR MODE II OPERATION

G_D : MODE II COMMAND SHAPING NETWORK. $G_D(s) = \frac{K(S+2.74)}{(S+20)(S+30)}$ $K = 40.2$

ITS REALIZATION IS AS FOLLOWS:

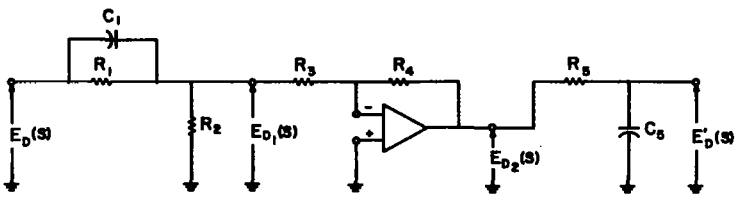

$C_1 = 1\mu f$
$R_1 = 0.3645\ M\Omega$ $R_3 = 1\ M\Omega$ $R_5 = 0.091\ M\Omega$
$R_2 = 0.03645\ M\Omega$ $R_4 = 3.67\ M\Omega$ $C_5 = 1\mu f$

SA : SUMMING AMPLIFIERS

FIGURE 13b. IDENTIFICATION OF ELEMENTS IN FLAPERON SERVOACTUATOR

MODE I SHAFT POSITION RESPONSE TRANSFER FUNCTION

$$\frac{\theta}{e} = \frac{207.43}{S} \frac{(S+22.5)(S+35)(S+225)}{(S+45)(S+P_1)(S+P_2)(S+P_3)} \quad \frac{\text{radians}}{\text{volt}}$$

P_1, P_2, P_3 are given in the last three columns of Table III

MODE I MOTOR VOLTAGE TRANSFER FUNCTION

$$\frac{e_m}{e} = \left(\frac{207.43}{726}\right) \frac{(S+Z_1)(S+Z_2)(S+22.5)(S+35)(S+225)}{S(S+45)(S+P_1)(S+P_2)(S+P_3)}$$

Z_1	Z_2	$\bar{K}/J$
0	24.2	0
1.88	22.32	42
12.1 + 4.65j	12.1 − 4.65 j	168

MODE I MAXIMUM EXCITATION

$$e = \frac{28}{S}$$

FIGURE 13c. SYSTEM TRANSFER FUNCTIONS FOR MODE I EXCITATION

MODE II SHAFT POSITION RESPONSE TRANSFER FUNCTION

$$\frac{\theta}{e} = 207.43 \left[\frac{40.2\,(S+2.74)}{(S+11)(S+30)}\right] \frac{(S+22.5)(S+35)(S+225)}{(S+45)(S+P_1)(S+P_2)(S+P_3)} \quad \frac{\text{radians}}{\text{volt}}$$

NOTE: quantity in brackets is transfer function of signal shaping network used in aircraft control system. Pilot input (represented by Mode II maximum excitation) passes first through this shaping network before encountering servo system terminals.

MODE II MOTOR VOLTAGE TRANSFER FUNCTION

$$\frac{e_m}{e} = \frac{207.43}{726} \left[\frac{40.2(S+2.74)}{(S\ 11)(S\ \ 30)}\right] \frac{(S+Z_1)(S+Z_2)(S+22.5)(S+35)(S+225)}{(S+45)(S+P_1)(S+P_2)(S+P_3)}$$

MODE II MAXIMUM EXCITATION

$$e = \frac{9.33\,(12.8)(S+20)}{S(S+12.8+9.6j)(S+12.8-9.6j)}$$

FIGURE 13d. SYSTEM TRANSFER FUNCTIONS FOR MODE II EXCITATION

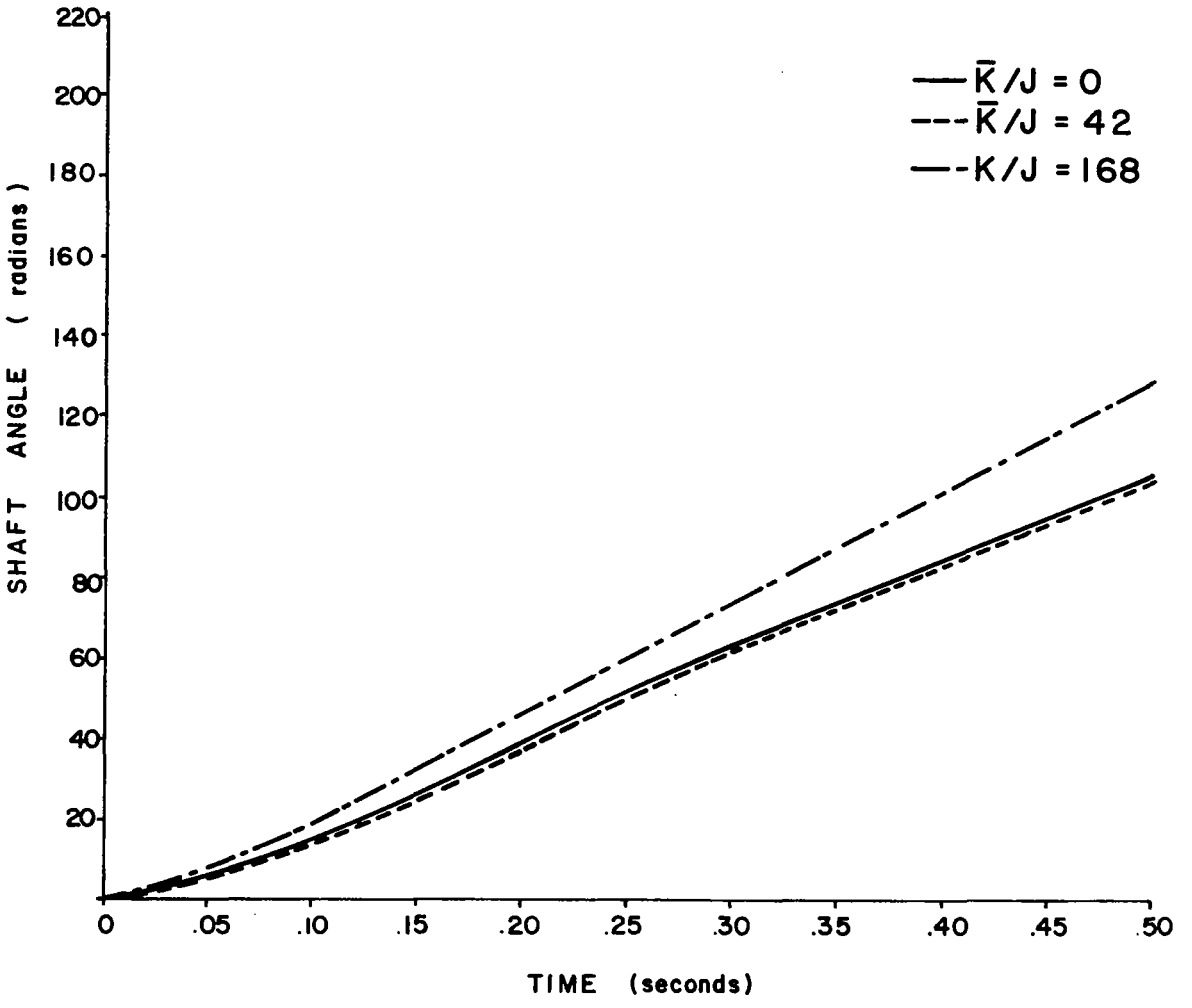

FIGURE 14. SYSTEM RESPONSE FOR A MODE I INPUT
(a). SHAFT ANGLE

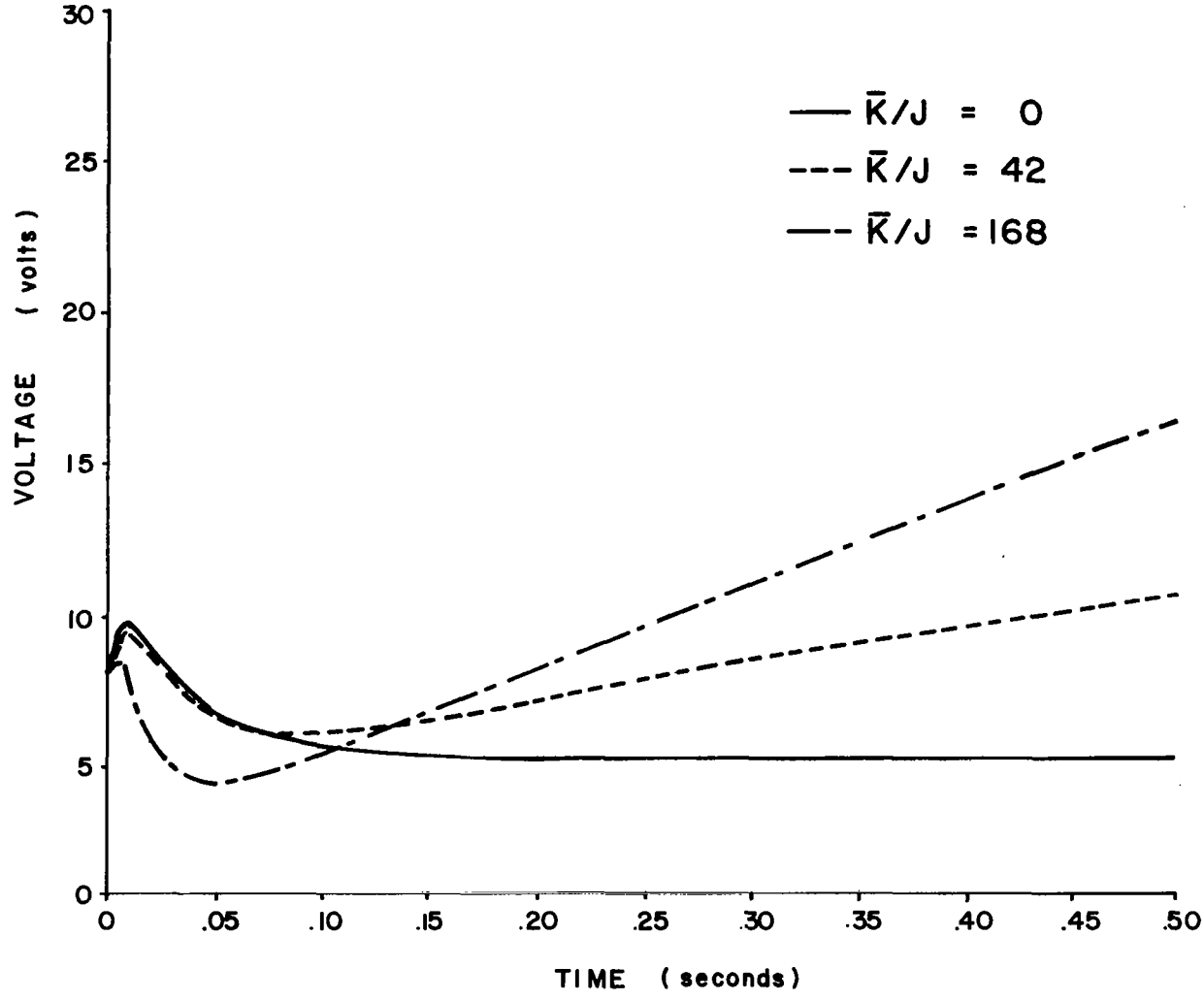

FIGURE 14. SYSTEM RESPONSE FOR A MODE I INPUT
(b). VOLTAGE

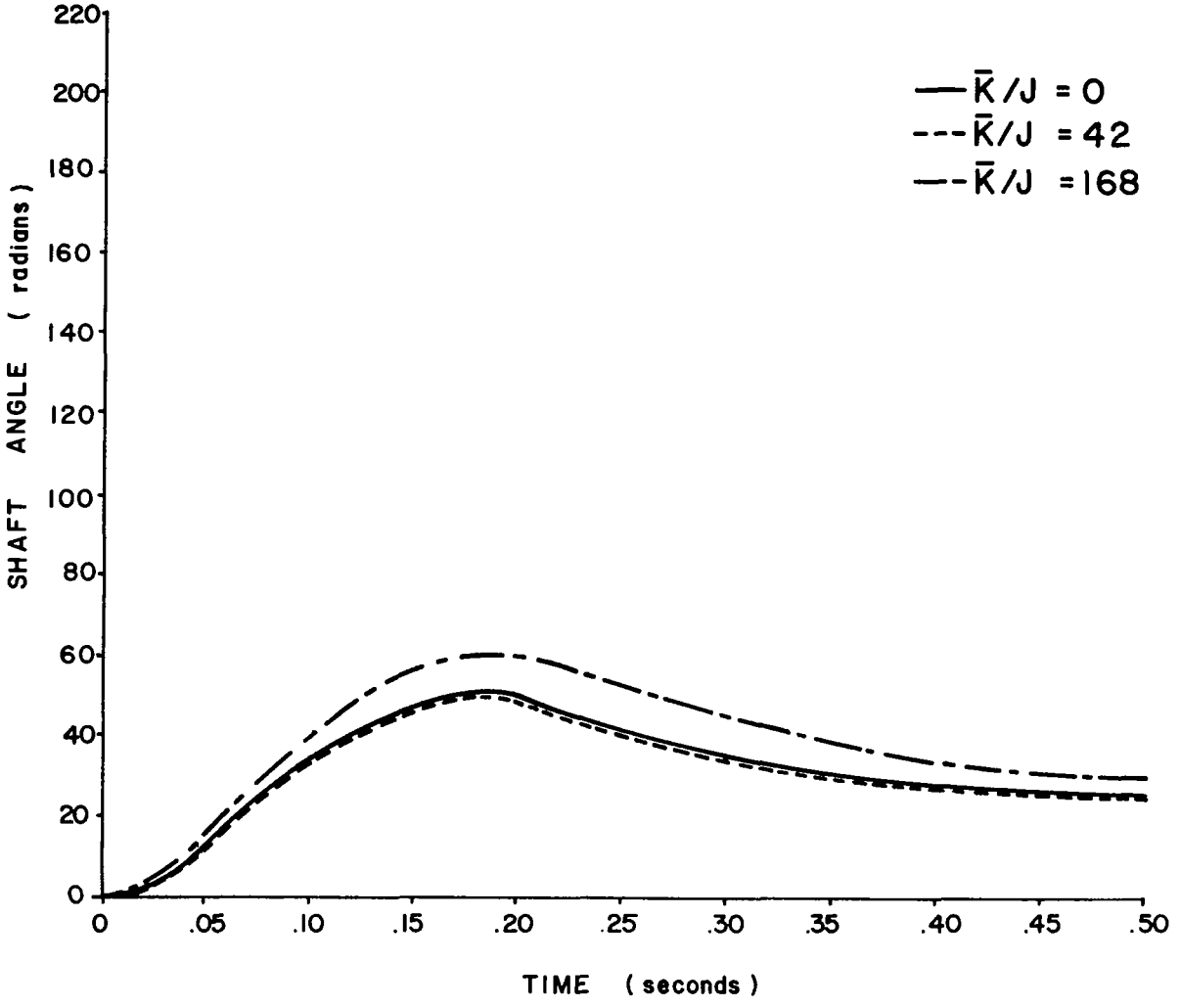

FIGURE 15. SYSTEM RESPONSE FOR A MODE II INPUT
(a). SHAFT ANGLE

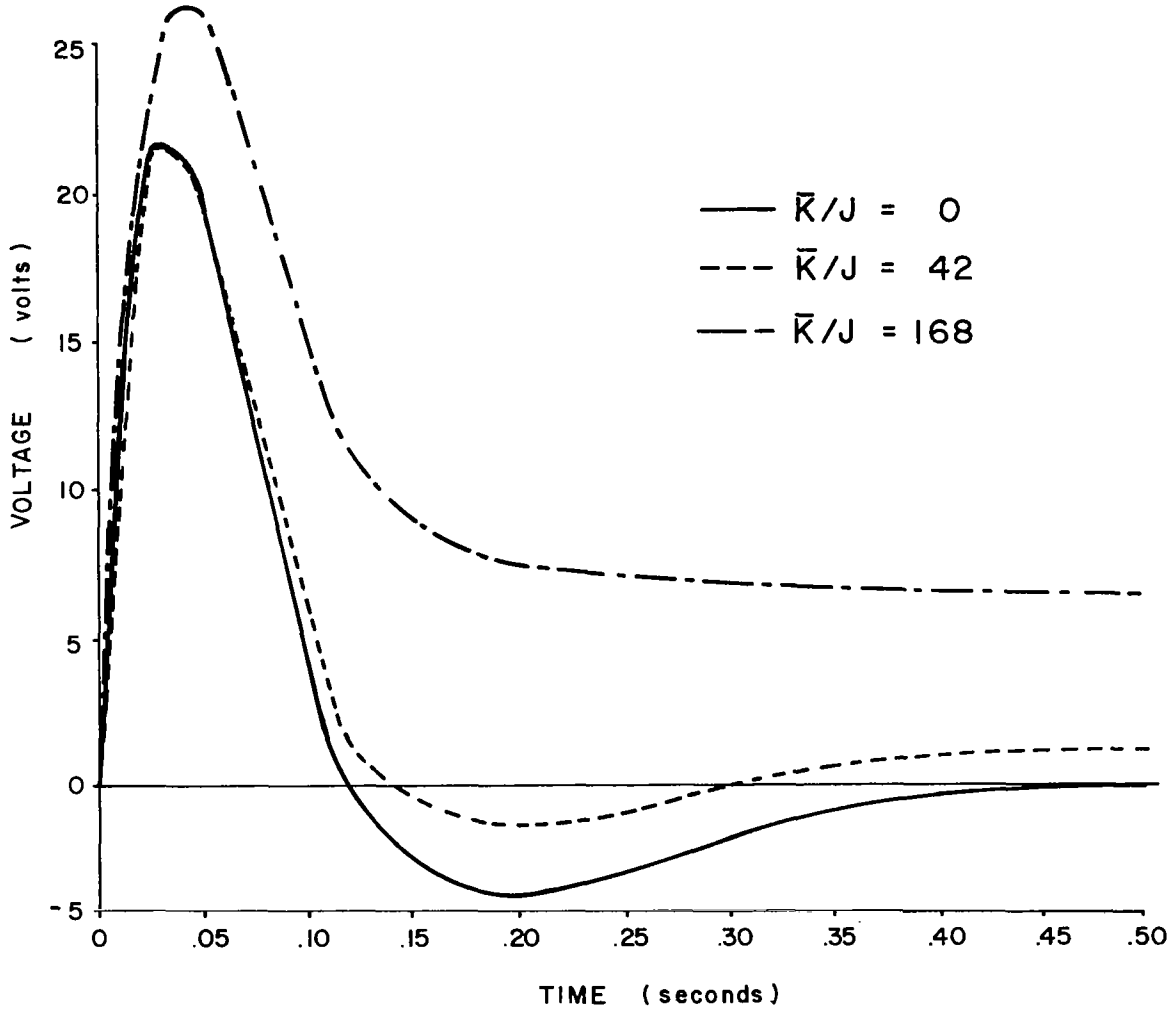

FIGURE 15. SYSTEM RESPONSE FOR A MODE II INPUT
(b). VOLTAGE

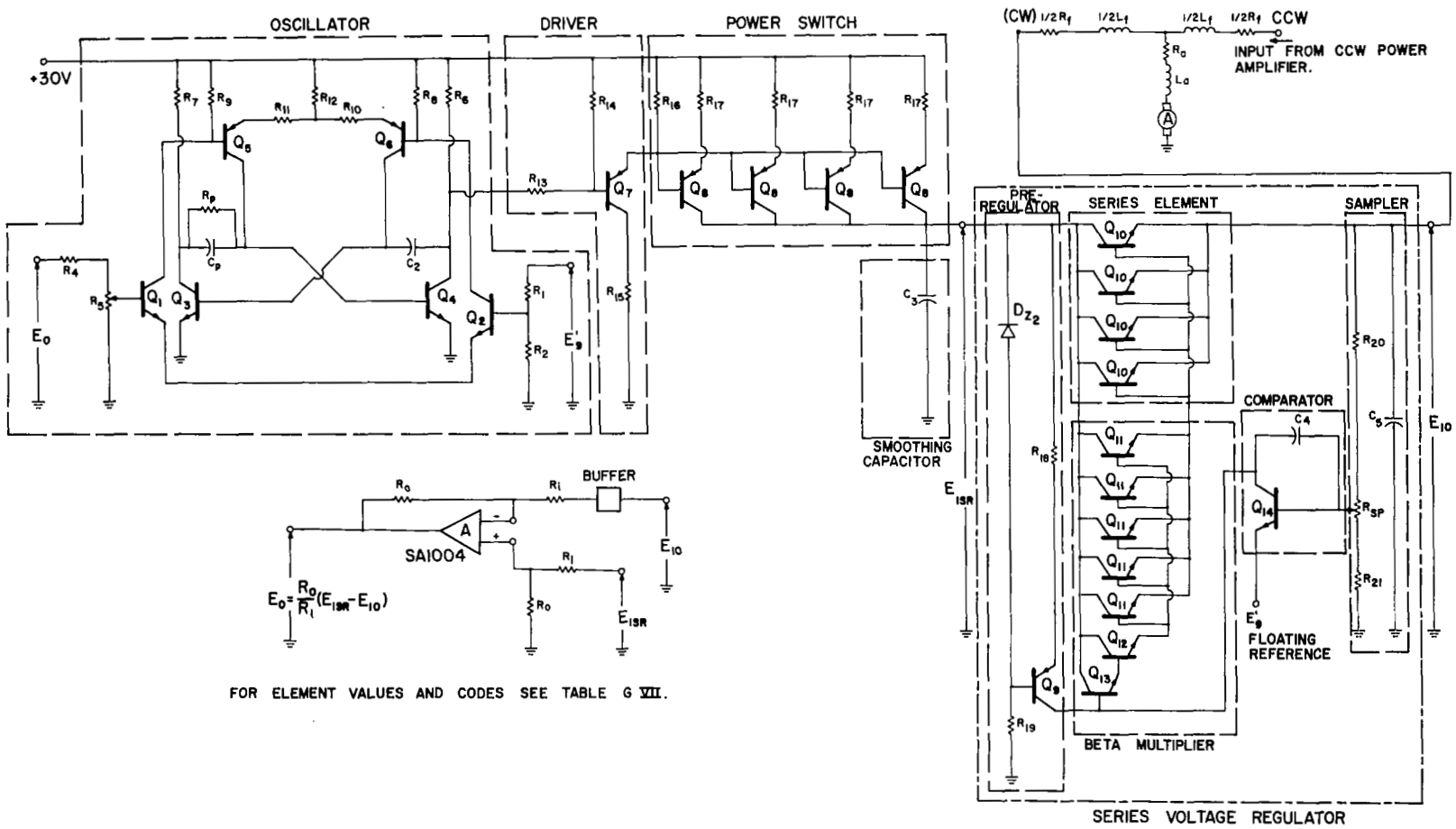

FOR ELEMENT VALUES AND CODES SEE TABLE G VII.

FIGURE 16. POWER AMPLIFIER SCHEMATIC

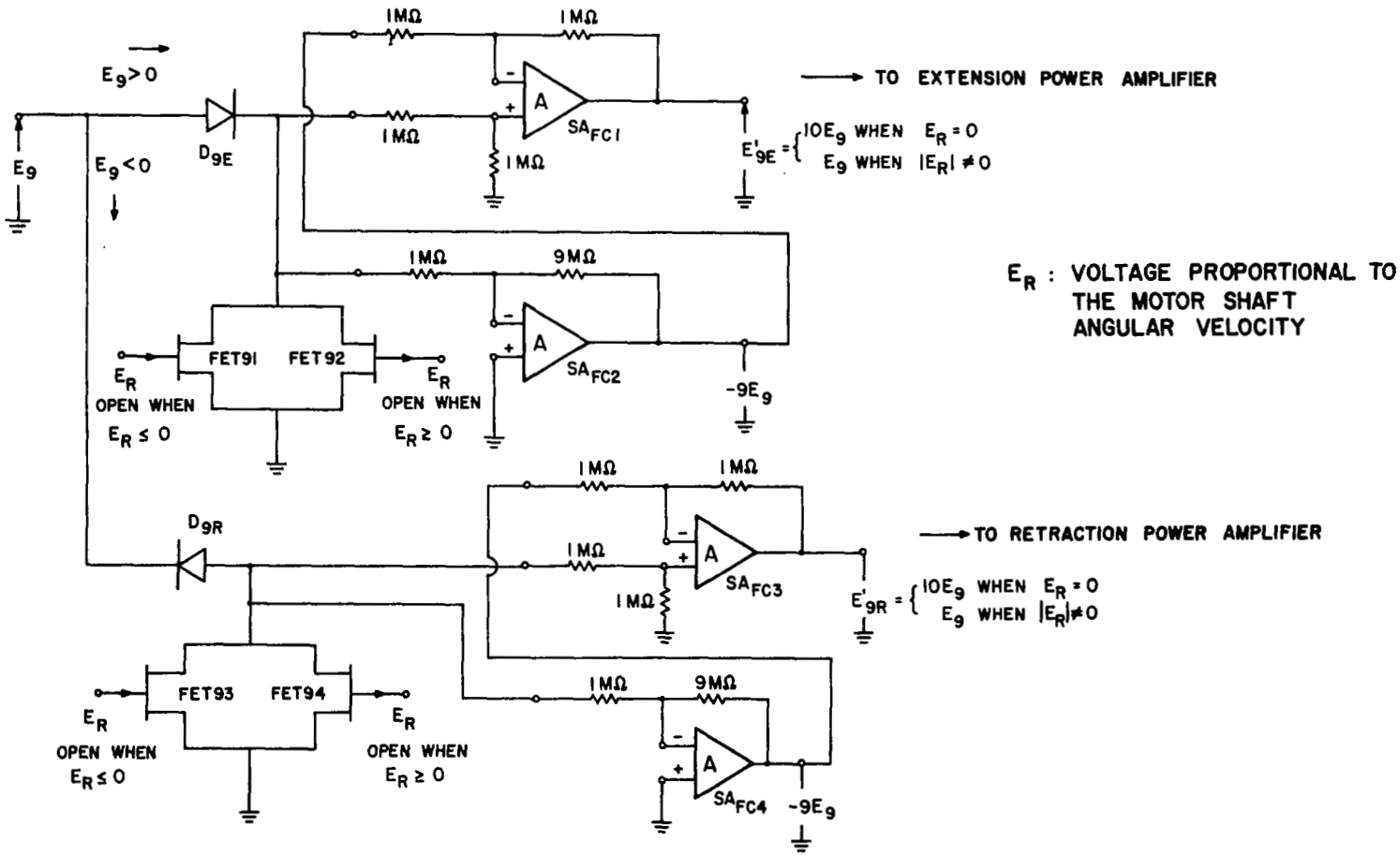

FIGURE 17. FRICTION COMPENSATOR SCHEMATIC

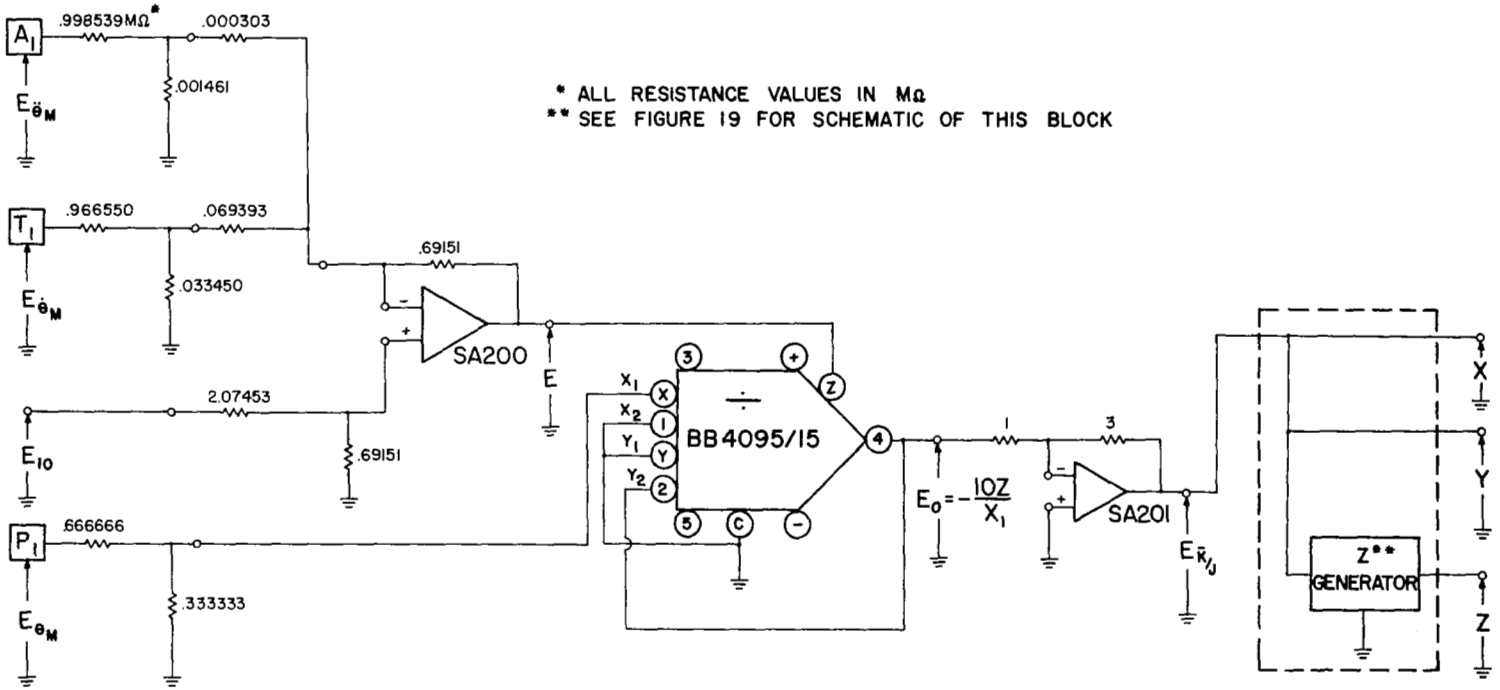

FIGURE 18. GENERATION OF VOLTAGES PROPORTIONAL TO $\frac{\bar{K}}{J}$

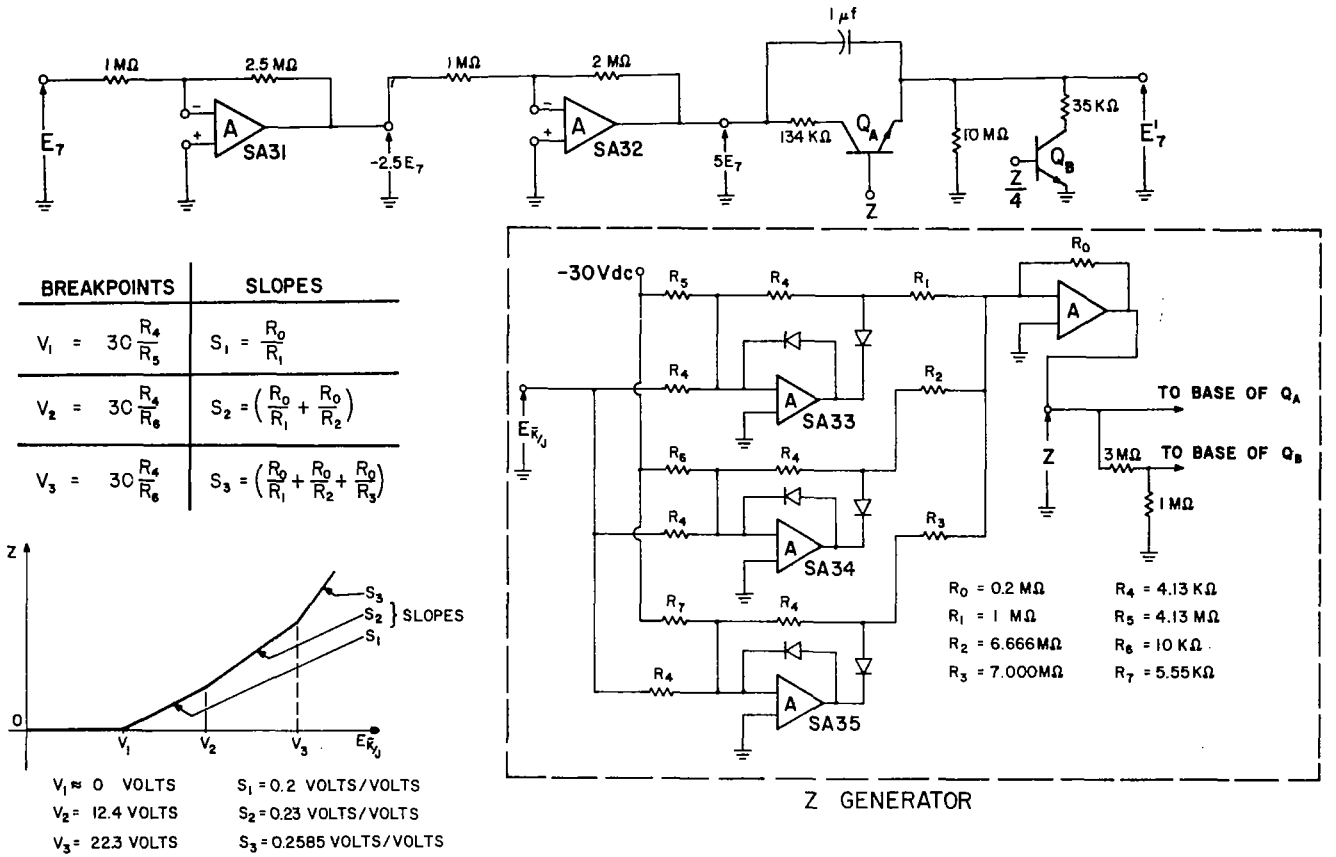

FIGURE 19. SCHEDULED LEAD COMPENSATOR

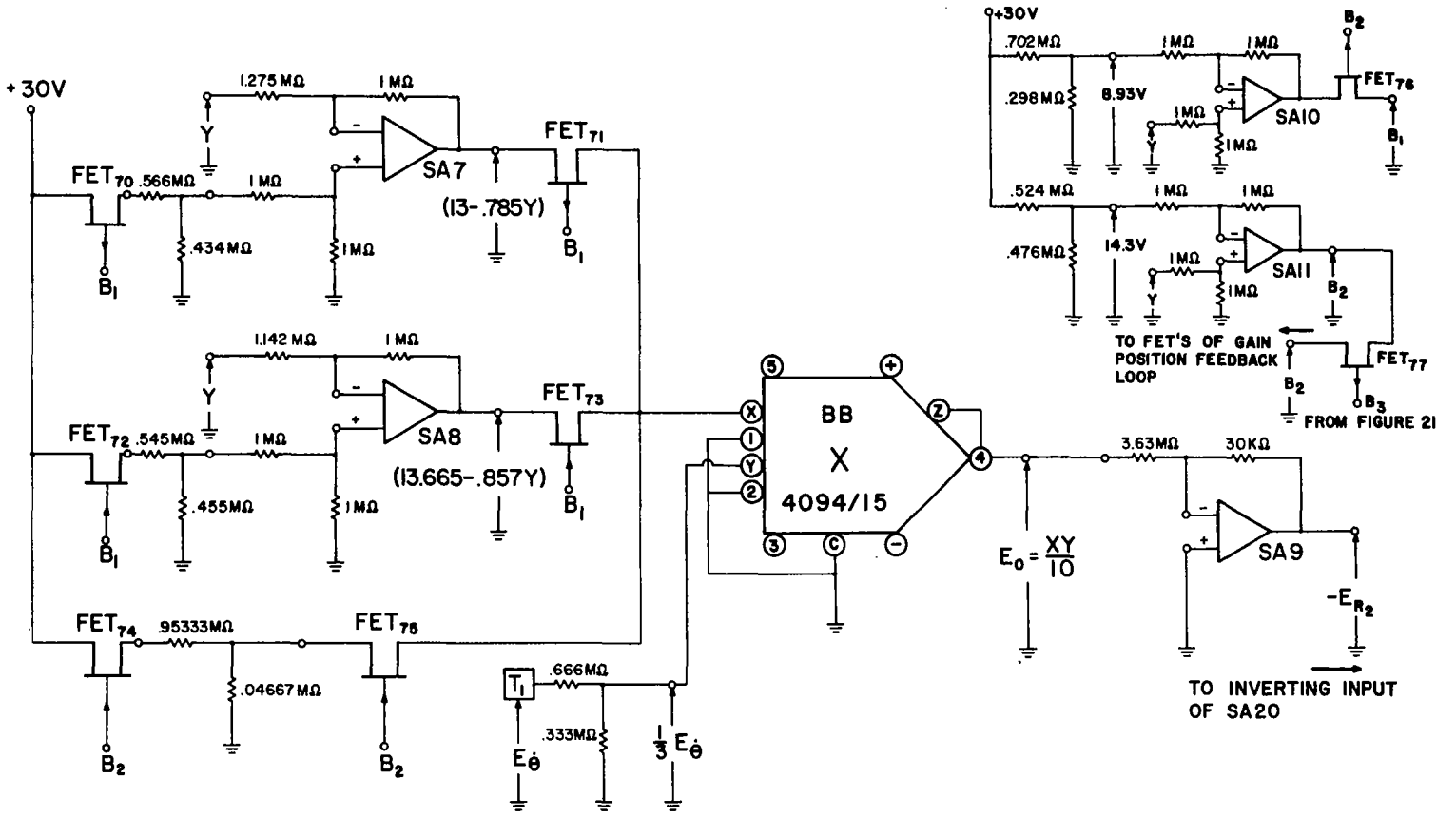

FIGURE 20. REALIZATION OF GAIN-SCHEDULED RATE FEEDBACK LOOP

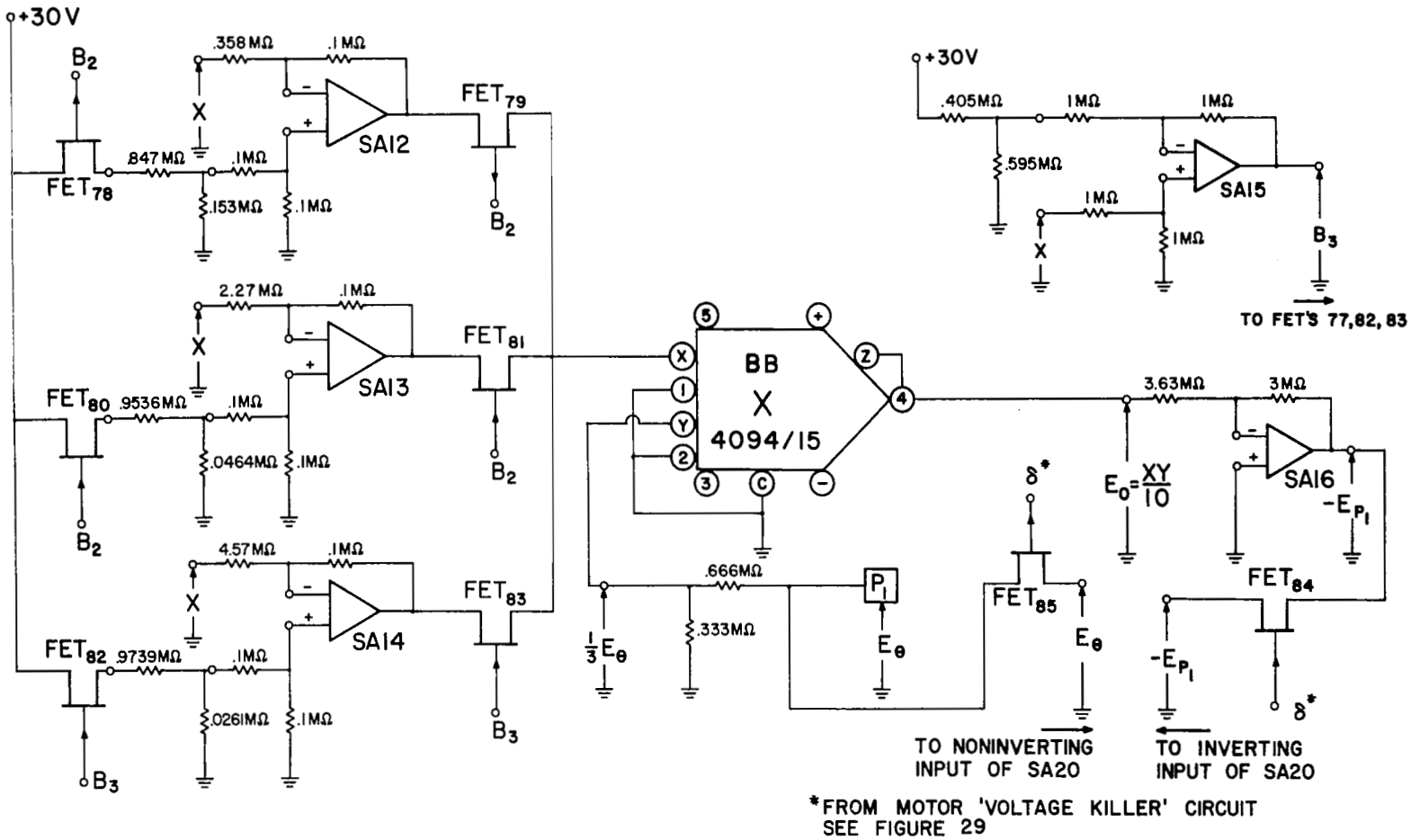

FIGURE 21. REALIZATION OF GAIN-SCHEDULED POSITION FEEDBACK LOOP

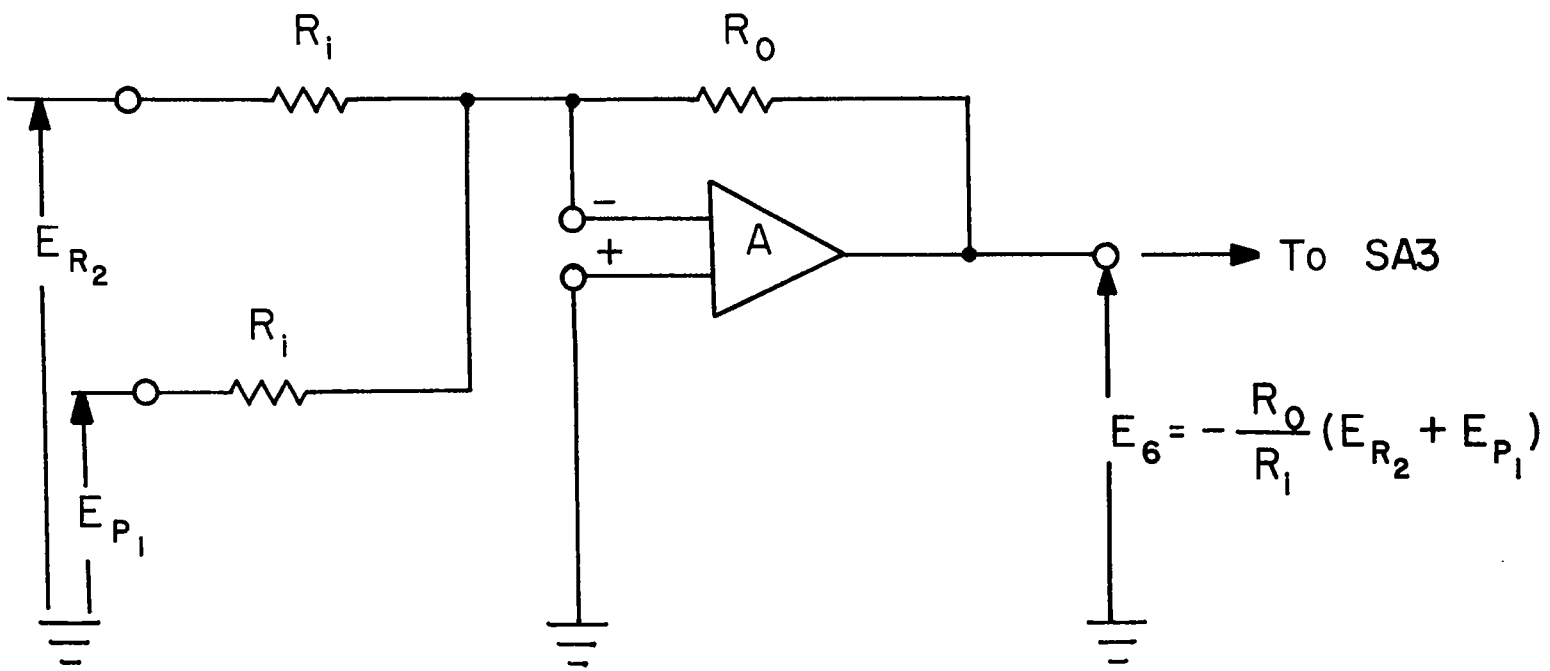

$R_o = R_i = 1\ M\Omega$

FIGURE 22. SUMMING AMPLIFIER SA20

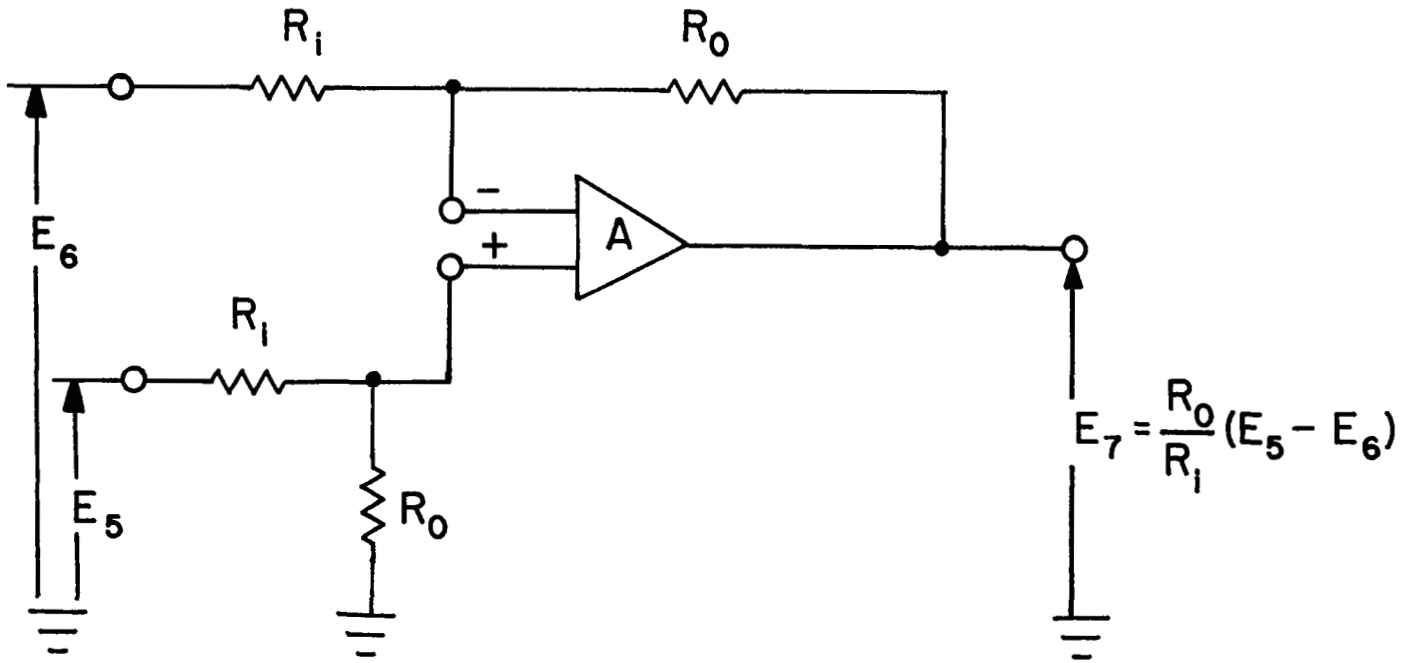

$R_0 = R_i = 1\ M\Omega$

FIGURE 23. SUMMING AMPLIFIER SA3

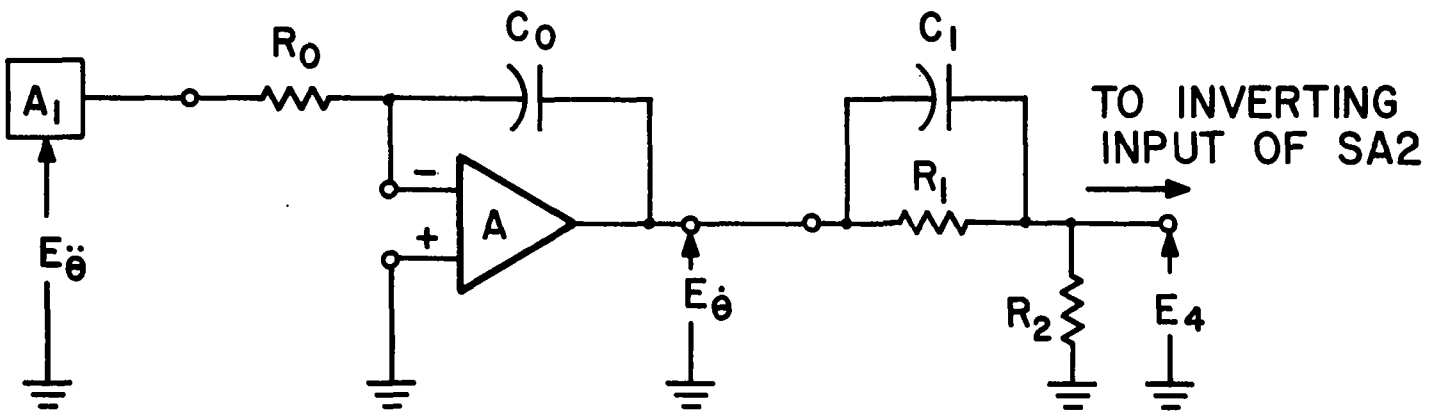

$C_0 = 10\mu f$

$R_0 = 5.2\ M\Omega$

$C_1 = 1\mu f$

$R_1 = 44.44\ K\Omega$

$R_2 = 4.83\ K\Omega$

$$H(s) = -\frac{70}{3630}\, S\, \frac{(S+22.5)}{(S+225)}$$

FIGURE 24. REALIZATION OF THE RESPONSE IMPROVEMENT LOOP

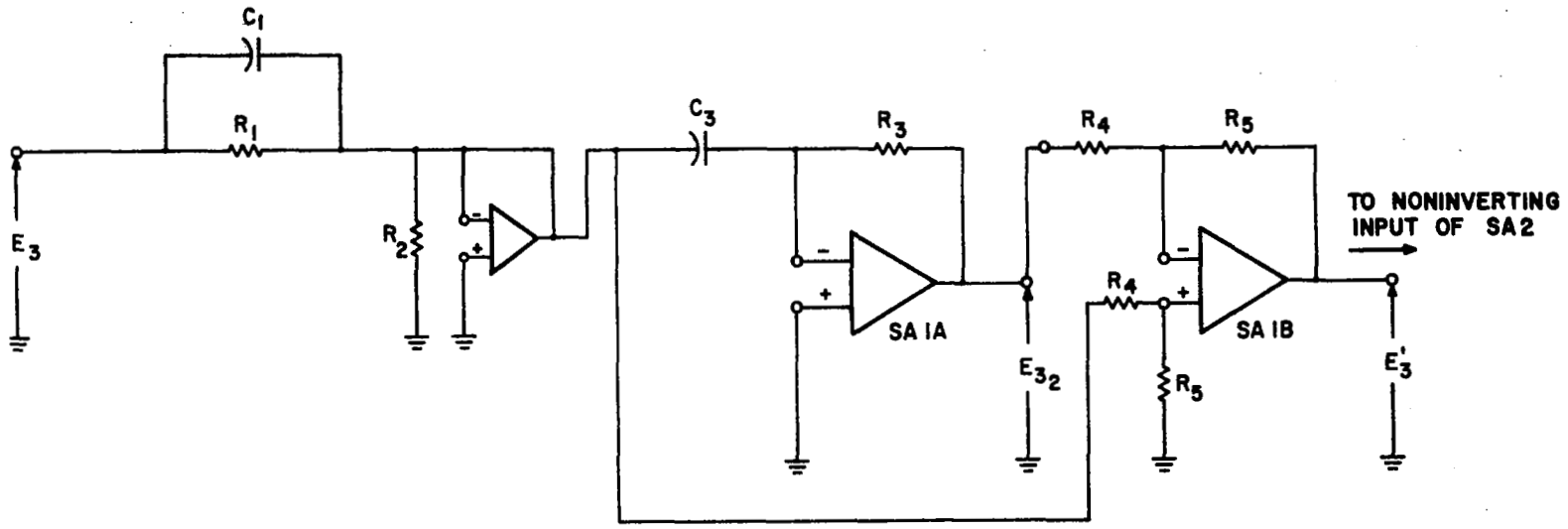

$C_1 = 1\mu f$

$R_1 = R_2 = 44.44K\Omega$

$C_3 = 1\mu f$

$R_3 = 28.6K\Omega$

$R_4 = 1M\Omega$

$R_5 = 2M\Omega$

$$C(s) = \left(\frac{S+22.5}{S+45}\right)\left(\frac{S+35}{17.5}\right)$$

FIGURE 25. REALIZATION OF THE FIXED EXTERNAL COMPENSATOR

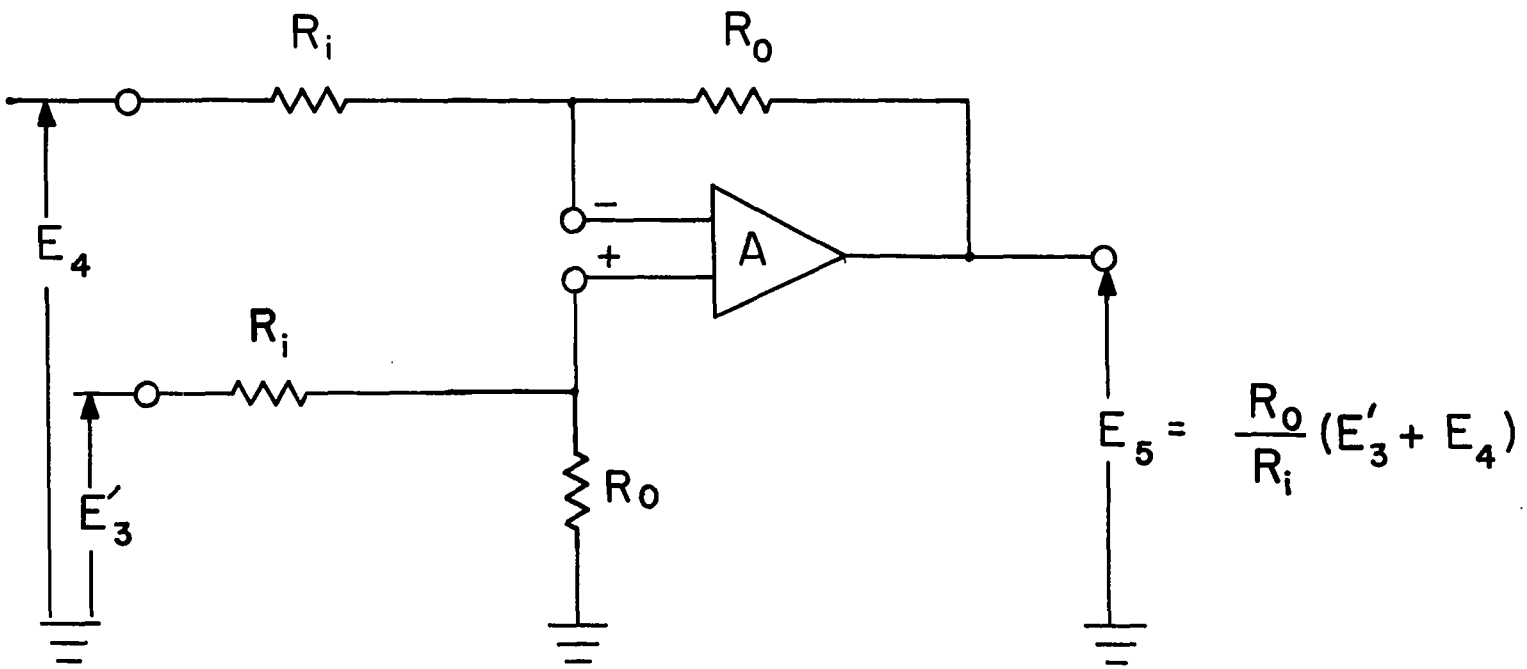

$R_0 = R_1 = 1\,M\Omega$

FIGURE 26. SUMMING AMPLIFIER SA2

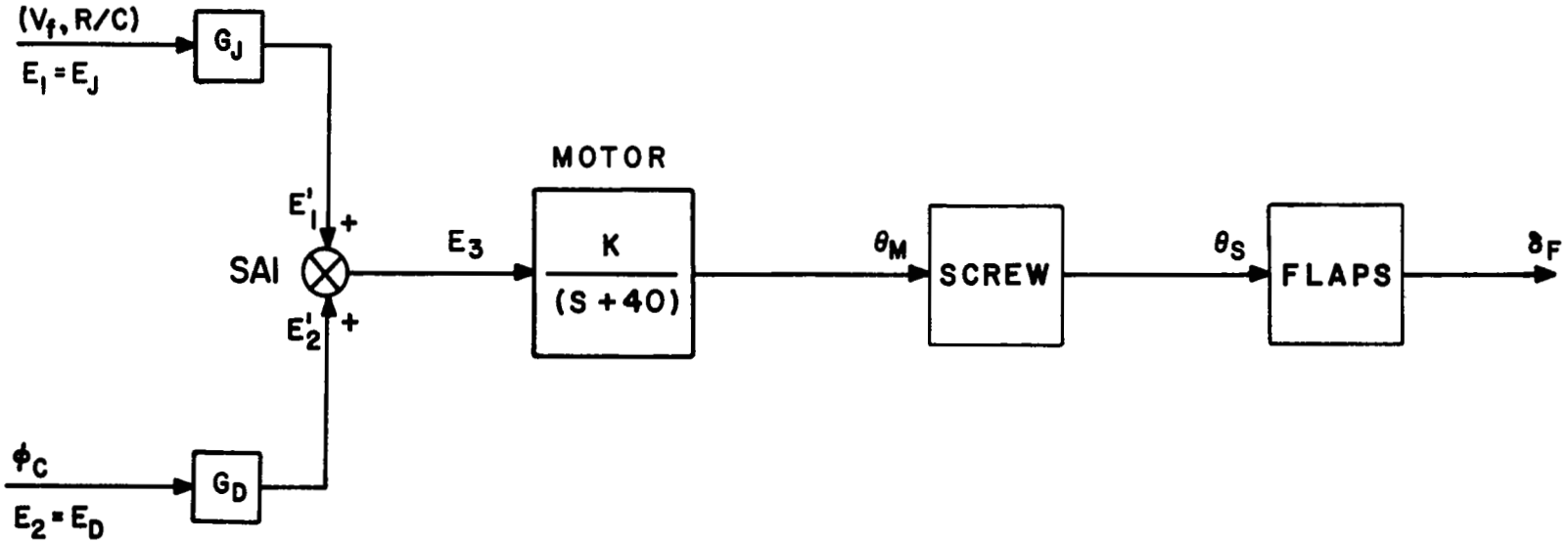

FIGURE 27. FINAL REDUCTION OF BLOCK DIAGRAM

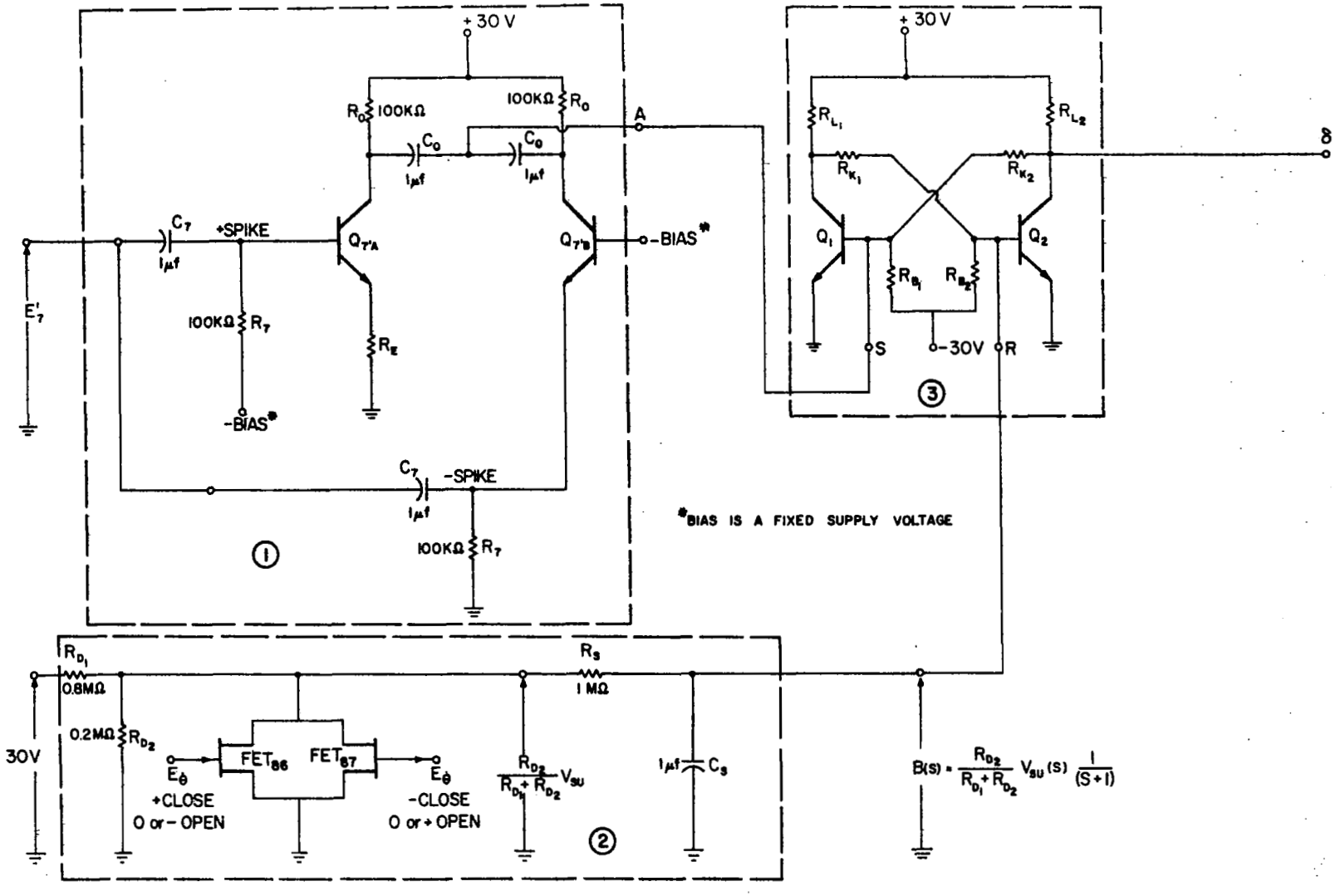

FIGURE 28. GENERATION OF VOLTAGE PULSE δ

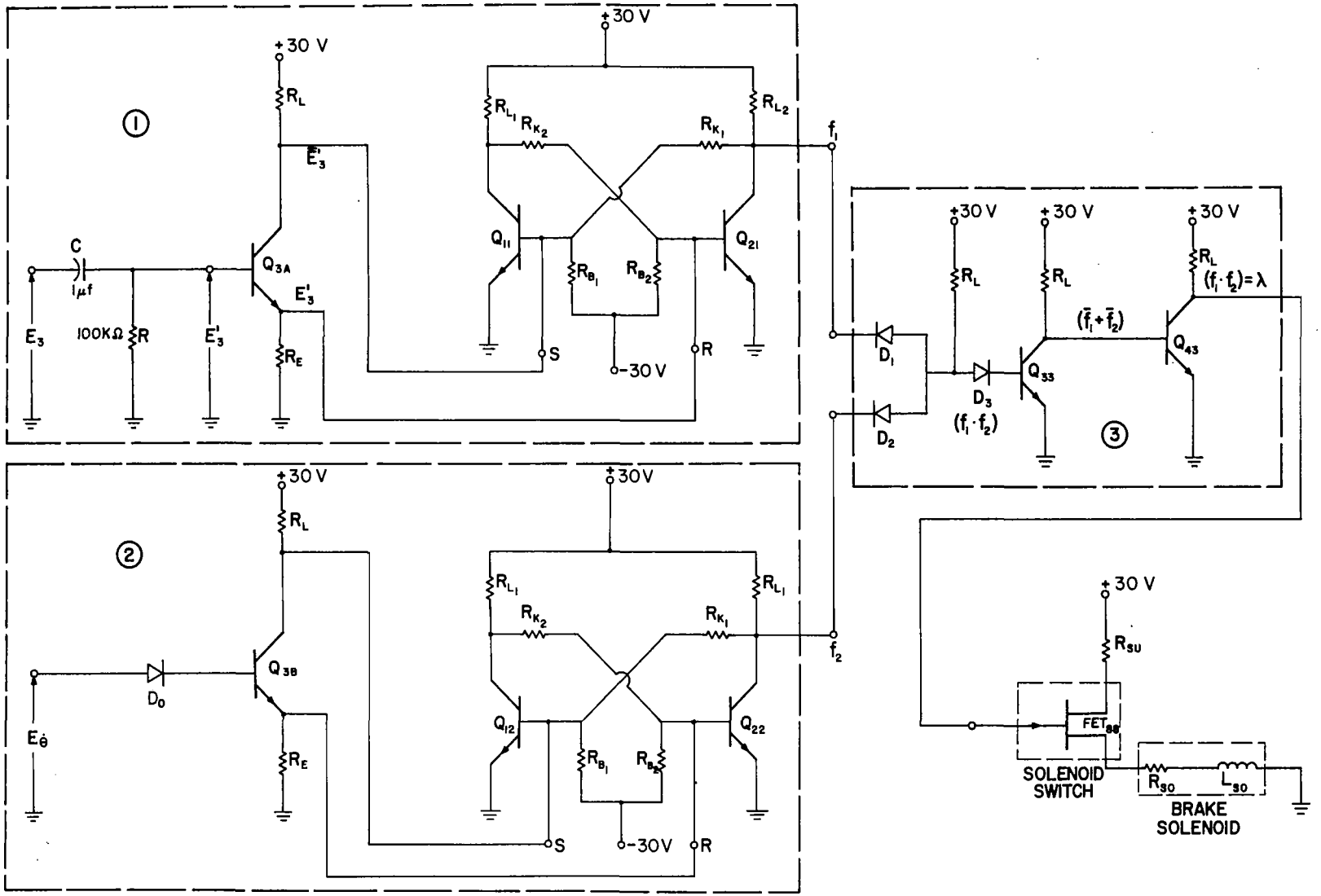

FIGURE 29. GENERATION OF VOLTAGE PULSE λ

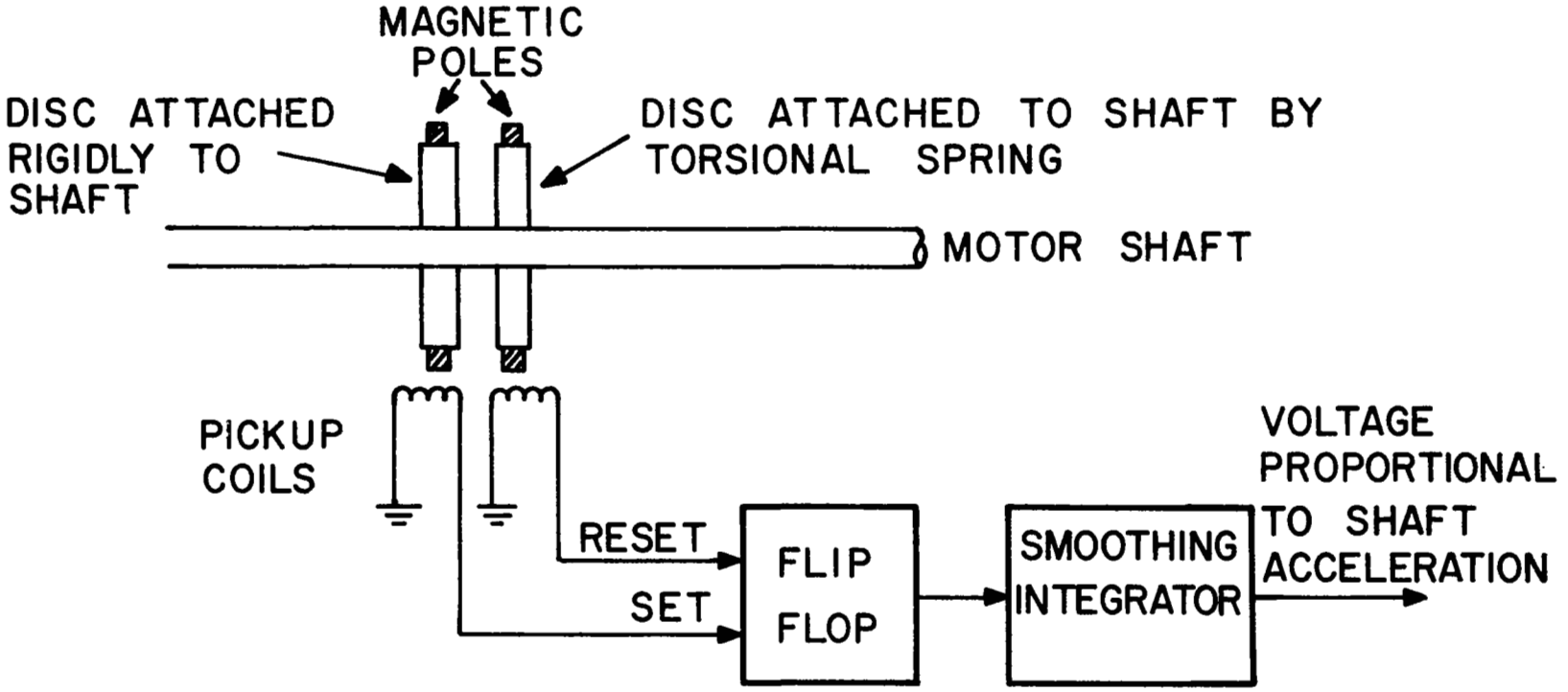

FIGURE 30. SCHEMATIC OF MOTOR SHAFT ACCELEROMETER

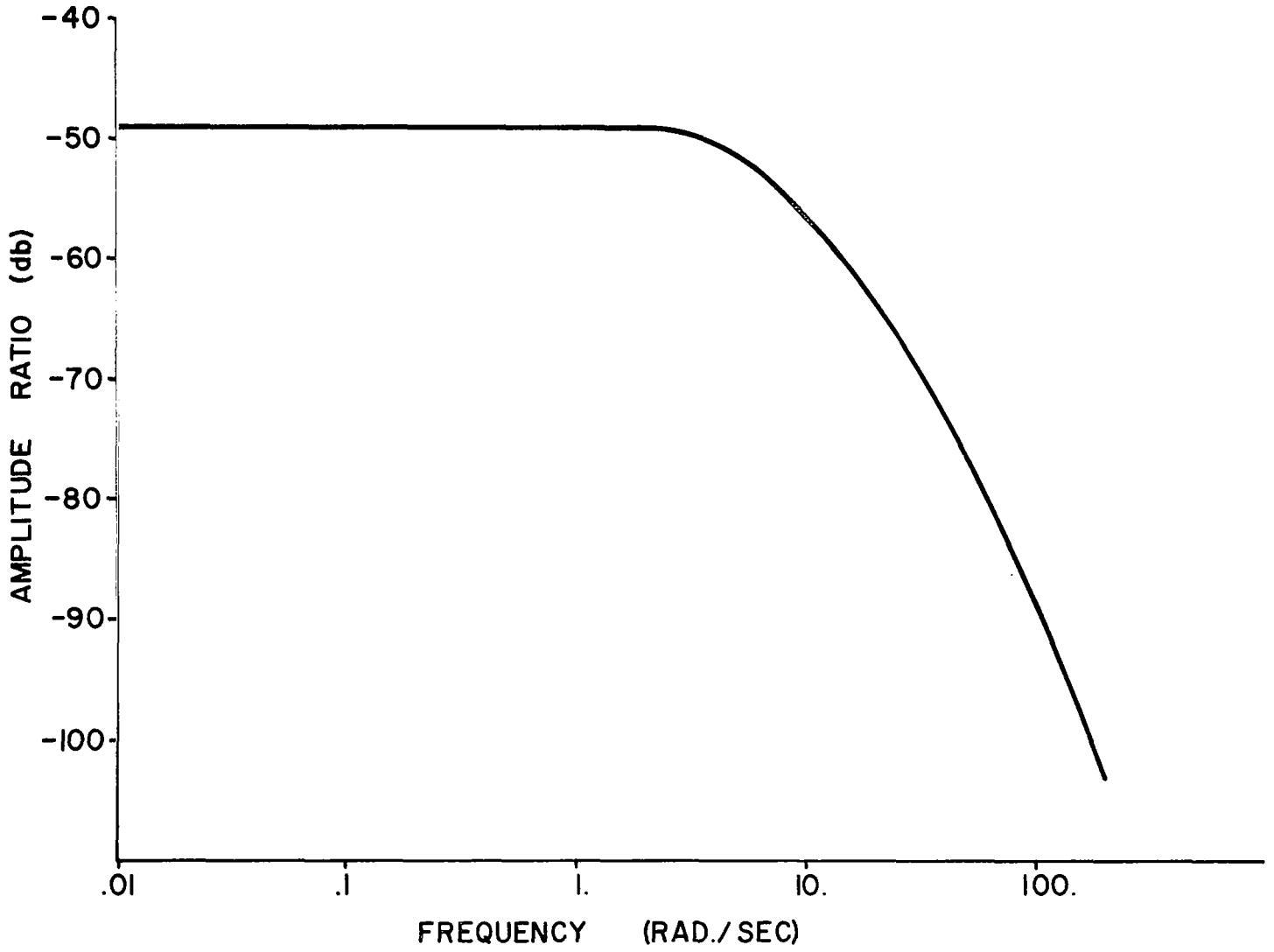

FIGURE 31. SYSTEM SHAFT ANGLE RESPONSE TO POTENTIOMETER SINUSOIDAL NOISE